PLOS ONE

RESEARCH ARTICLE

Environmental factors shaping bacterial, archaeal and fungal community structure in hydrothermal sediments of Guaymas Basin, Gulf of California

Gustavo A. Ramírez[1,2,3]*, **Paraskevi Mara**[4], **Taylor Sehein**[4], **Gunter Wegener**[5,6], **Christopher R. Chambers**[1], **Samantha B. Joye**[7], **Richard N. Peterson**[8], **Aurélie Philippe**[9], **Gaëtan Burgaud**[9], **Virginia P. Edgcomb**[4], **Andreas P. Teske**[1]

1 Department of Marine Sciences, University of North Carolina at Chapel Hill, NC, United States of America, 2 Department of Marine Biology, Leon H. Charney School of Marine Sciences, University of Haifa, Haifa, Israel, 3 College of Veterinary Medicine, Western University of Health Sciences, Pomona, CA, United States of America, 4 Geology and Geophysics Dept., Woods Hole Oceanographic Institution, Woods Hole, MA, United States of America, 5 MARUM, Center for Marine Environmental Sciences, University Bremen, Germany, 6 Max-Planck-Institute for Marine Microbiology, Bremen, Germany, 7 Department of Marine Sciences, University of Georgia, Athens, GA, United States of America, 8 School of Coastal and Marine Systems Science, Coastal Carolina University, Conway, SC, United States of America, 9 Univ. Brest, Laboratoire Universitaire de Biodiversité et Ecologie Microbienne, Plouzané, France

* ramirezg@westernu.edu

Abstract

The flanking regions of Guaymas Basin, a young marginal rift basin located in the Gulf of California, are covered with thick sediment layers that are hydrothermally altered due to magmatic intrusions. To explore environmental controls on microbial community structure in this complex environment, we analyzed site- and depth-related patterns of microbial community composition (bacteria, archaea, and fungi) in hydrothermally influenced sediments with different thermal conditions, geochemical regimes, and extent of microbial mats. We compared communities in hot hydrothermal sediments (75-100°C at ~40 cm depth) covered by orange-pigmented *Beggiatoaceae* mats in the Cathedral Hill area, temperate sediments (25-30°C at ~40 cm depth) covered by yellow sulfur precipitates and filamentous sulfur oxidizers at the Aceto Balsamico location, hot sediments (>115°C at ~40 cm depth) with orange-pigmented mats surrounded by yellow and white mats at the Marker 14 location, and background, non-hydrothermal sediments (3.8°C at ~45 cm depth) overlain with ambient seawater. Whereas bacterial and archaeal communities are clearly structured by site-specific *in-situ* thermal gradients and geochemical conditions, fungal communities are generally structured by sediment depth. Unexpectedly, chytrid sequence biosignatures are ubiquitous in surficial sediments whereas deeper sediments contain diverse yeasts and filamentous fungi. In correlation analyses across different sites and sediment depths, fungal phylotypes correlate to each other to a much greater degree than Bacteria and Archaea do to each other or to fungi, further substantiating that site-specific *in-situ* thermal gradients and geochemical conditions that control bacteria and archaea do not extend to fungi.

Introduction

In the Guaymas Basin spreading center, located in the central Gulf of California, hydrothermally influenced sediments are characterized by steep thermal gradients that may reach the thermal limits of life in just a few centimeters depth [1, 2]. The extreme temperatures transform buried organic matter into complex mixtures of dissolved inorganic carbon (DIC), methane, ammonia, organic acids, short chain alkanes, and aromatic compounds that migrate to shallow sediments and sustain diverse and active microbial communities [3–6].

Among the surface expressions of hydrothermalism, microbial mats are widespread and conspicuous [7] and provide visual markers for hydrothermally active sediments poised for sampling by submersible [2]. Previous works in Guaymas Basin have explored the ecophysiology and genomics of mat-building filamentous sulfur-oxidizing *Beggiatoaceae* lineages [8–13], and investigated the effects of high temperature and hydrothermally influenced geochemistry as local ecological constraints on microbial community structure in the underlying sediments [14, 15]. These sediments harbor complex anaerobic microbial communities, including diverse methanogens [16], thermophilic or thermotolerant archaea that oxidize methane and short-chain alkanes [15, 17–21] and hydrocarbon-oxidizing, free-living or syntrophic sulfate-reducing bacteria (reviewed by [22]). In metagenomic surveys of mat-covered hydrothermal sediments, oxygen- or nitrate-reducing, chemosynthetic Gamma- or Epsilonproteobacteria occur at the sediment surface whereas the sediment column is dominated by functionally and phylogenetically diverse uncultured, anaerobic bacteria and archaea [23, 24].
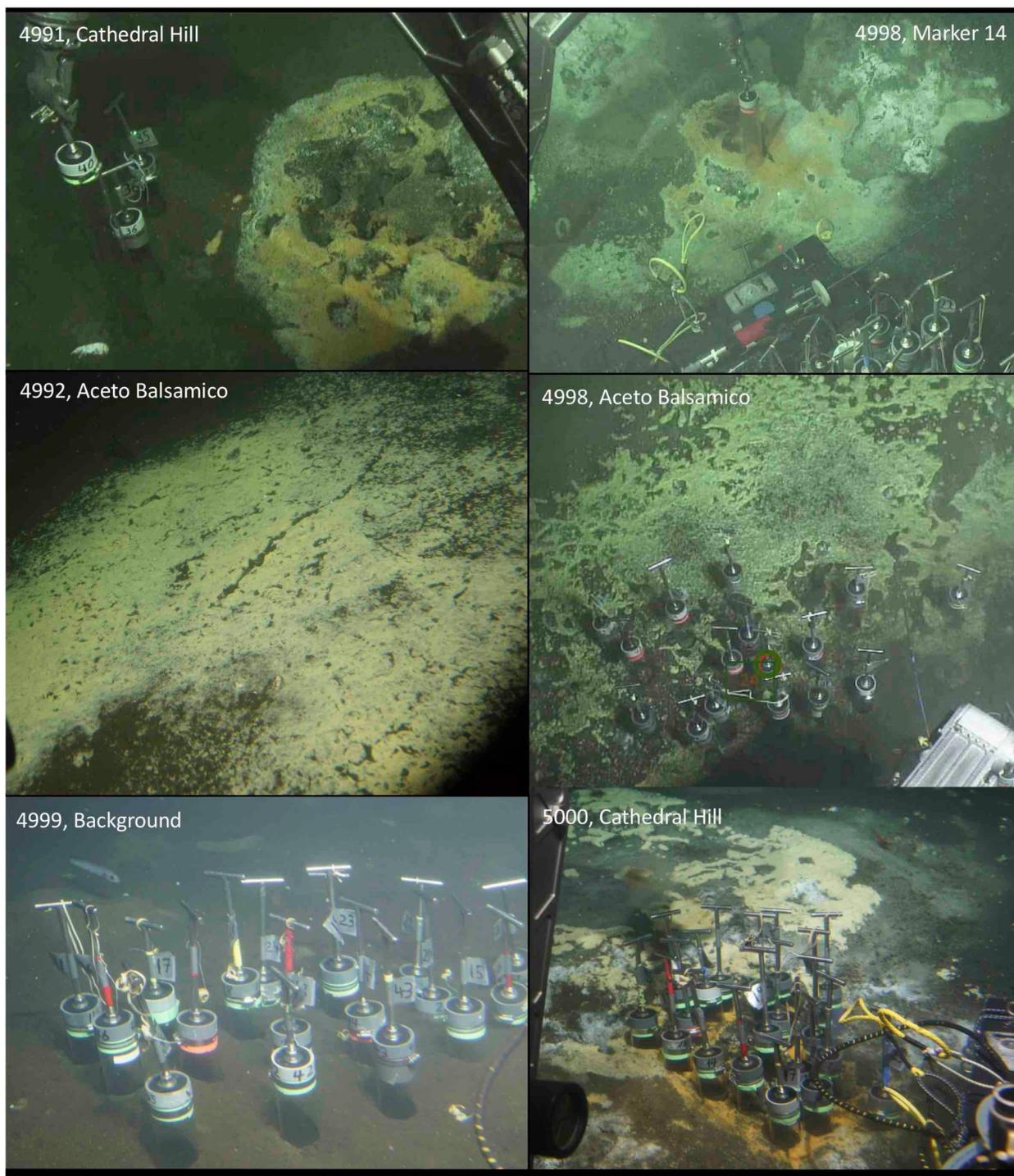
Despite the growing body of knowledge describing how the environment influences bacterial and archaeal community structuring in Guaymas Basin, little is known about the environmental controls on fungal diversity and distribution patterns. Fungal studies in Guaymas Basin sediments are so far limited to initial sequence-based [25, 26] and small-scale cultivation studies [27]. To explore environmental controls on fungal diversity and occurrence patterns, and fungal associations with bacteria and archaea, we analyzed site- and depth-related patterns of bacteria, archaea and fungi in hydrothermally influenced sediments of Guaymas Basin under different thermal and geochemical regimes retrieved from four different locations: i) hot hydrothermal sediments covered by orange-pigmented *Beggiatoaceae* mats in the Cathedral Hill area, ii) temperate sediments covered by yellow sulfur precipitates and filamentous sulfur oxidizers at the Aceto Balsamico location [2], iii) hot sediments with orange-pigmented mats surrounded by yellow and white mats at the Marker 14 location [14], and iv) bare background sediments with ambient seawater temperatures at a nearby control site (Fig 1, S1 Fig in S1 File). Previous investigations in Guaymas Basin have shown that sediment temperature affects *Beggiatoa* mat heterogeneity [9], limits methane and short-chain alkane oxidation and organic matter remineralization in hydrothermal sediments [14, 15] and cold seeps [28]; further, site-specific environmental histories can influence ecological structuring [29]. Overall, these studies suggest that bacterial and archaeal communities are predominantly structured by *in-situ* thermal and geochemical regimes.

To broaden our understanding of microbial processes in hydrothermally influenced sediments and to identify potential interactions between bacteria, archaea and fungi, we examined environmental controls on fungal communities in the context of parallel analyses of bacteria and archaea from the same sample set, keeping in mind that these controls are likely to change between surficial and subsurface sediments. Specifically, we investigated whether fungal communities in Guaymas Basin follow similar thermal and biogeochemical controls as bacteria and archaea, or are structured differently, perhaps stochastically or by co-occurrence with other microbiota.

Material and methods

Field survey and sampling

Guaymas Basin sites were visited and sampled with R/V *Atlantis*, HOV *Alvin* and AUV *Sentry* during cruise AT42-05 (Nov. 15–29, 2018). *Alvin* dives targeted previously explored sampling

Fig 1. Sampling sites. In-situ photographs of sampling sites in the southern axial valley of Guaymas Basin. Courtesy of *Alvin* group, WHOI.

https://doi.org/10.1371/journal.pone.0256321.g001

Table 1. *Alvin* cores. Metadata for sediment cores sampled for bacterial, archaeal and fungal community composition (B, A, F), and only fungal community composition (F). Temperatures are mid-point approximations for top, middle and bottom sediment layers in each core.

Dive & Core	Sampling area	Latitude/longitude	Depth in m	Mats	Slicing scheme in cm intervals	community composition	Approx. thermal range
4991–10 4991–12	Cathedral Hill	27.0114/-111.4045	2014	Orange	0–6, 6–12, 12–18	B, A, F	16/33/45˚C
4991–37 4991–38	Cathedral Hill	27.0114/-111.4045	2014	Bare	0–10,10–20,20–30	F	5/8/10˚C
4991–42 4991–43	Cathedral Hill	27.0114/-111.4045	2014	White/ orange	0–10,10–20,20–30	F	8/12/17˚C
4992–22 4992–23	Aceto Balsamico	27.0081/-111.4071	2012	Yellow	0–10, 10–20	B, A, F	6/9˚C
4994–07 4994–09	Cathedral Hill	27.0114/-111.4045	2014	Orange	0–7, 7–14, 14–21 Surf., 0–7, 7–14	F	8/14/18˚C 3/8/14˚C
4998–13 4998–18	Marker 14	27.0079/-111.4072	2011	Orange	0–7, 7–14, 14–21	B, A, F	12/33/60˚C
4998–19 4998–21	Aceto Balsamico	27.0078/-111.4071	2011	Yellow	0–10,10–20,20–30	B, A, F	5/9/13˚C
4999–17	Background	27.0069/-111.4066	2014	Bare	0–5, 5–10, 10–15	B, A, F	3/3/3˚C
5000–11 5000–20	Cathedral Hill	27.0122/-111.4039	2009	Orange	0–7, 7–14, 14–21	B, A, F	23-33/44-69/74-86˚C

https://doi.org/10.1371/journal.pone.0256321.t001

areas [2] that were mapped in additional detail by AUV Sentry. Photo coverage of *Alvin* dives is available at the *Alvin* frame-grabber site [http://4dgeo.whoi.edu]. The bathymetry of the hydrothermally active graben segment in southern Guaymas Basin had been mapped previously by AUV *Sentry* during dives 407–409 and 413–417 in 2016 (S1 Fig in S1 File) from a height of 65–70 meters above bottom [30]. Push cores of approx. 12" or 16" (30 to 40 cm) length were collected during *Alvin* dives 4991 to 5001, returned to the surface, and sampled in the shipboard laboratory within a few hours. Sampling site data are summarized in Table 1.

Thermal profiles

Thermal profiles were measured in surficial sediments using *Alvin's* 50 cm heat flow probe (https://ndsf.whoi.edu/alvin/using-alvin/sampling-equipment/). The 50 cm probe has thermal sensors every 10 cm, starting 5 cm under the attached plastic disk (the "puck") that limits probe penetration and rests on the seafloor once the probe is inserted. After approx. 3 to 5 minutes, temperature readings stabilize and are recorded. The heat flow probe shorted at the beginning of *Alvin* dive 5000; instead, the thermosensor within the tip of the suction intake was inserted into the sediment at approx. 5 cm, 10 cm and 20 cm depth, and the temperature was recorded immediately. Thermal profiles adjacent to sediments used in this study are compiled in Table 2.

Porewater geochemistry

For porewater analysis, intact sediment cores were sampled using Rhizons (Rhizosphere Research Products, Wageningen, NL) as described previously [31]. The overlying water was removed from the cores and holes were drilled at designated sediment sampling horizons. Rhizons washed with hydrochloric acid (1M) and deionized water were injected through these holes, and vacuum was applied with syringes for approx. 30 min to collect porewater samples. The sediment interval depths are given in Table 1. For sulfide analysis, 1 ml of the collected

Table 2. Thermal profiles. *Alvin* temperature measurements with heatflow probe (Dives 4991, 4992, 4998, 4999) and one-point T-sensor (Dive 5000). Sediment depths for T-sensor measurements during Dive 5000 were estimated by the *Alvin* pilot.

Alvin Dive	4991			4992	4994	4998				4999	5000		
Temp. Profile				T3		T1	T2	T9	T10		T1	T2	T3
Mats	orange	none	white	yellow	orange	orange		yellow		none	orange		
Nearby cores	10 to 12	35 to 40	41 to 45	18 to 24	7, 9	11 to 18		19 to 27		14 to 24	8 to 23		
0 cm	3.8–5.0	3.4–5.4	3.3–4.4	3.0–3.5	n.d.	n.d.	n.d.	n.d.	n.d.	n.d	n.d.	n.d.	n.d.
5 cm	14.0	4.6	7.9	5.7	5	12.4	15.8	5.0	5.6	3.2	20.6	23	33
10 cm	28.9	6.7	9.3	7.3	10.4	33.3	32.8	7.3	8.0	n.d.	44	53	69
15 cm	56.4	8.0	11.6	9.2	n.d.	53.7	50.9	8.6	8.7	n.d.	n.d.	n.d.	n.d.
20 cm	48.9	9.0	14.0	11.0	n.d	74.1	69.3	10.7	11.0	n.d.	74	80	86
25 cm	55.8	9.9	17.2	12.7	26	92.2	88.2	12.5	12.4	n.d.	n.d.	n.d.	n.d.
30 cm	59.9	10.6	20.3	14.4	n.d.	110.4	107.6	14.8	14.7	n.d.	n.d.	n.d.	n.d.
35 cm	66.0	12.1	23.4	16.0	n.d.	>115	>115	17.3	17.0	n.d.	n.d.	n.d.	n.d.
40 cm	72.7	13.1	26.8	17.8	n.d.	>115	>115	19.5	19.5	n.d.	n.d.	n.d.	n.d.
45 cm	79.8	13.7	31.0	19.7	48	>115	>115	21.7	21.2	3.9	n.d.	n.d.	n.d.

https://doi.org/10.1371/journal.pone.0256321.t002

porewater samples were fixed with 0.1 ml 0.1 M zinc acetate solution. Porewater samples were frozen at -20˚C for storage and shipping.

At the Max-Planck-Institute for Marine Microbiology (Bremen, Germany), samples were homogenized and sulfide concentrations were determined photometrically using the methylene blue method in 2 ml assays [32]. For sulfate measurements, the same samples were diluted in water (1:50) and analyzed using ion chromatography (Metrohm 930 Compact IC flex with Metrosep A PCC HC/4.0 preconcentration column, and Metrosep A Supp 5 Guard/4.0 chromatography column). The porewater concentrations of ammonium, phosphate, nitrate/nitrite and silicate were determined using a continuous flow nutrient analyzer (QuAAtro39; Seal Analytical) as published previously [33]. These data are compiled in the (S1 Table in S1 File) and are also documented online [34].

As a complement to Rhizon sampling, additional geochemical analyses were performed on centrifuged porewaters and sediments from three layers per core (surface, middle, bottom) of 6–10 cm each (Table 1). Sediment cores were sampled in 3 cm intervals. Sediment samples of ca. 40 ml were centrifuged in 50 ml conical Falcon tubes under nitrogen for 5 to 10 minutes at 1000 g, resulting in the separation of 8 to 10 ml porewater from the sediment. For porewater sulfide analysis, 1 ml porewater subsamples were drawn into syringes, filtered immediately through 0.45 µm filters, and placed in Eppendorf sample vials each containing 0.1 ml of 0.1 M zinc acetate solution to preserve the sulfide as stable zinc sulfide precipitate until analyzed. Sulfide was quantified spectrophotometrically at UNC-Chapel Hill using the methylene blue method [32]. For sulfate analysis, 1 ml porewater samples were immediately acidified with 50 microliters of 1 N HCl and bubbled with N_2 for 1 minute to remove hydrogen sulfide. After returning the samples to the home laboratory, sulfate concentrations were determined using the ion chromatograph of the UNC Environmental Program (S2 Table in S1 File). At Louisiana State University Wetland Biogeochemistry Analytical Services (WBAS), colorimetric determinations of ammonium, nitrate, soluble reactive phosphorus and total phosphorus were performed using a OI Analytical Flow Solutions IV auto analyzer, and sediment total nitrogen and carbon (weight %) were measured with a Costech 1040 CHNOS Elemental Combustion system (S3 Table in S1 File). Filtered porewater samples were analyzed for dissolved organic carbon (DOC) and total dissolved nitrogen (TDN) using a Shimadzu TOC/TN analyzer. Dissolved organic nitrogen (DON) was calculated by subtracting TDN from the sum of the inorganic nitrogen species (S3, S4 Tables in S1 File).

For methane measurements, sediment samples of 2 ml were collected from freshly recovered cores using cut-off syringes, and transferred into serum vials supplemented with 1 ml of 1M NaOH which were stoppered with thick blue butyl rubber stoppers and crimp-sealed. Methane $\delta^{13}C$ isotope values from headspace gas samples were measured using a Finnigan-MAT DeltaPlus Stable Light Isotope Ratio Monitoring Mass Spectrometer in the Organic Mass Spectrometry Facility at WHOI. Values are reported in the per mil (‰) notation relative to Vienna Pee Dee Belemnite (VPDB) (S5 Table in S1 File).

DNA extraction, amplification and sequencing

Freshly recovered sediment cores were divided into three layers (near-surface, middle, bottom) of 6 to 10 cm thickness each (Table 1) for DNA extraction and sequence-based analysis. This approach covered the available thermal range of cored sediment, while providing sufficient material for coordinated experiments with other cruise participants, and accommodating temperature fluctuations due to pulsating hydrothermal flows that impact surficial (5 to 10 cmbsf) sediments [14]. Total DNA was extracted using the FastDNA^TM Spin Kit for Soil (MP Biomedicals), as recommended for marine sediment [35], following the manufacturer's protocol. Bacterial and archaeal SSU rRNA hypervariable region 4–5 (V4-V5) amplicons were generated using the 515F-Y (5′-GTGYCAGCMGCCGCGGTAA-3′) and 926R (5′-CCGYCAATTYMTT TRAGTTT-3′) primers and customized thermocycling parameters [36]. Fungal ITS2 region amplicons were generated using the 5.8S-Fun (5′-AACTTTYRRCAAYGGATCWCT-3′) and ITS4-Fun (5′-AGCCTCCGCTTATTGATAT-GCTTAART-3′) primers and customized thermocycling parameters [37]. All amplicons were generated and sequenced at Georgia Genomics and Bioinformatics Core, University of Georgia, using Illumina MiSeq PE 300 chemistry.

Bioinformatics analyses

Bacterial, archaeal and fungal gene sequence analyses were performed using the DADA2 package [38] implemented directly in R and QIIME2, respectively. Briefly, for bacterial and archaeal 16S rRNA genes, forward and reverse reads were trimmed with the filterAndTrim() command using the following parameters: trimLeft = c(20,20), maxEE = c(2,2), rm. phix = TRUE, multithread = TRUE, minLen = 130, truncLen = c(290,200). Error assessments and independent forward and reverse read de-replication were performed. Sequencing errors were removed to better infer the composition of the samples using the dada() command and, subsequently, error-free forward and reverse reads were merged using the mergePairs() command, specifying overhand trimming and a minimum overlap of 150 base pairs. Bacterial and archaeal 16S rRNA gene Amplicon Sequence Variants (ASVs) were assigned taxonomy using the SILVA 132 database [39]. For fungal ITS rRNA and 18S rRNA gene analyses, DADA2 was implemented in QIIME2 [40]. Fungal ASVs were assigned taxonomy by BLAST against the UNITE (v.8.0 2018-11-18) classifier [41]. Taxonomy assignments and count tables were merged with metadata as S4 objects for ordination analyses (PCoA) and data visualization in R using the phyloseq [42]), vegan [43], and MASS [44] packages. Further information on methods and ASV numbers is documented in S2 Fig and S6 Table in S1 File.

Taxonomy notes

The classification scheme as implemented in the SILVA 132 database [39] is currently changing. For example, genomics-based taxonomy revisions have raised the Epsilonproteobacteria to phylum status [Epsilonbacteraeota, [45]] and reorganized the Deltaproteobacteria into several phylum-level lineages [46]. Since the taxonomic landscape continues to evolve, we use designations that are currently widely shared, in particular phylum-level archaeal designations

that have gained widespread usage during the ongoing rapid expansion of the archaeal domain [for example Bathyarchaeota, [47, 48]]. Roadmaps for achieving consistent taxonomy of the cultured and uncultured microbial world have been proposed recently [49].

Network analyses

To visualize the relationships between archaeal, bacterial and fungal ASVs within the targeted sediment samples, network analyses were performed using Calypso [50] and MetagenoNets [51] web-tools. The 23591 ASVs were Hellinger-transformed, filtered to 84 ASVs using a minimum prevalence of 0.03 and an occurrence of 5, and subjected to network analysis for identification of co-occurring and mutually exclusive taxa using the CCREPE (Compositionality Corrected by Renormalization and Permutation) algorithm [51, 52] Taxa are represented as nodes, taxa abundance is shown as node size, and significant edges, based on Pearson's critical r correlations, represent positive (blue) and negative (red) associations that we utilize for assisting with data interpretation and hypothesis generation. Complementary heatmaps were also processed using MetagenoNets.
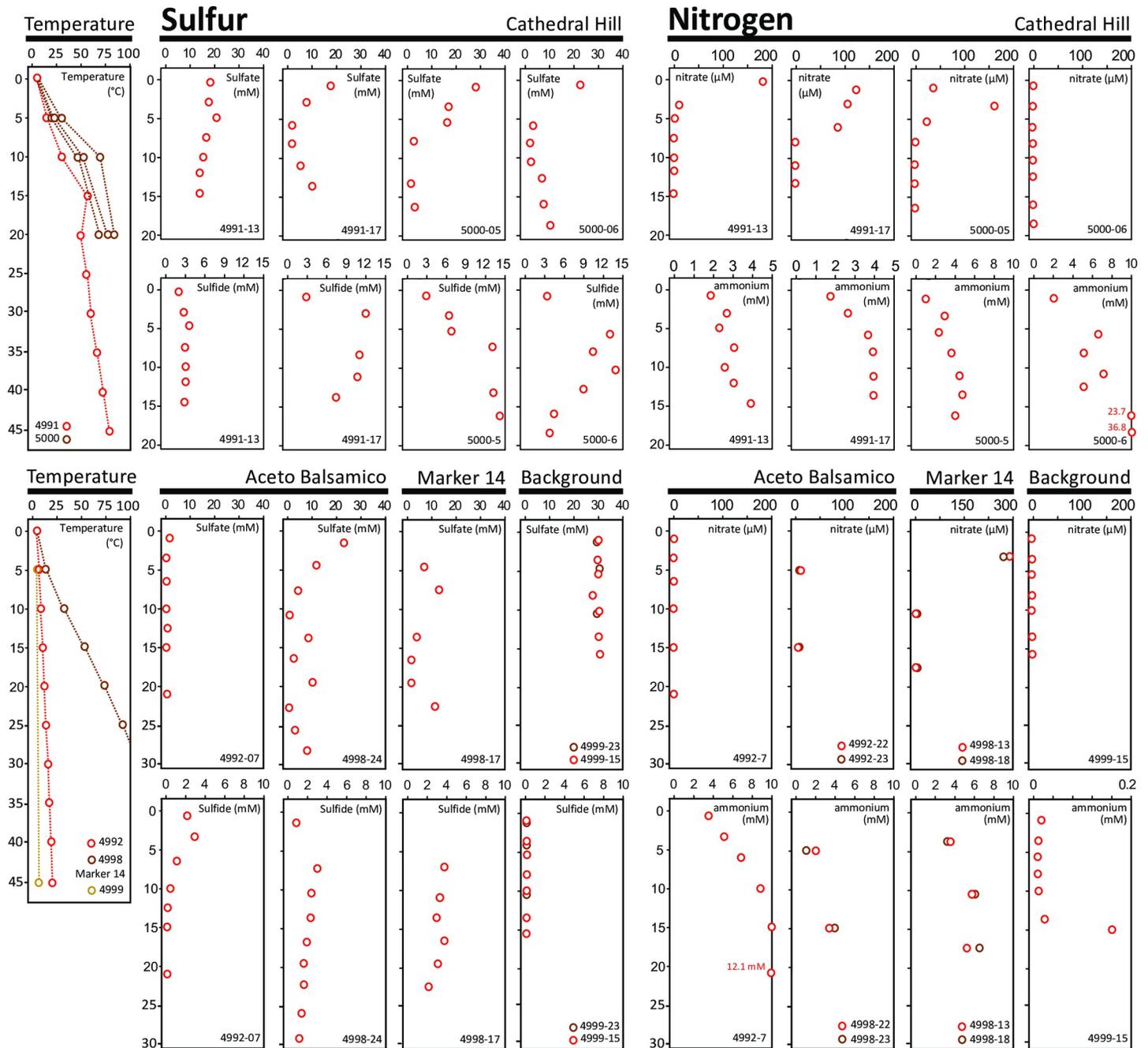
Results

Guaymas Basin survey sites

During expedition AT42–05 to Guaymas Basin (Nov. 15–29, 2018), AUV *Sentry* re-surveyed the bathymetry of the southern Guaymas Basin trough [30] and submersible *Alvin* sampled hydrothermally active sediments. Different types of mat-covered sediments (Table 1) and thermal regimes (Table 2) were sampled at the Cathedral Hill, Aceto Balsamico, Marker 14 and Background locations.

At Cathedral Hill, gradually sloping sediment-covered mounds with extensive hydrothermal areas and white, yellow and orange microbial mats (Fig 1) are topped with large hydrothermal edifices [2]. The Cathedral Hill area was targeted for push-core sampling of high-temperature microbial mats by submersible *Alvin*. These hydrothermal sediments show rapidly increasing temperatures with depth that reach up to 75 to 100°C within 30 to 40 cm from the sediment-water interface (Fig 2). Push cores from hydrothermal sediments with orange mats of filamentous *Beggiatoaceae* are characterized by sulfate replenishment below the sediment surface (Fig 2), most likely by seawater inmixing and active hydrothermal circulation [2, 14]. Interestingly, nitrate in concentrations of 100 to 200 µM appears in surficial sediment of several cores, a possible consequence of entraining seawater and nitrate-accumulating filamentous *Beggiatoaceae* [13]. Consistent with previous analyses of Guaymas Basin hydrothermal fluids [3] and sediments [13], the hydrothermal Cathedral Hill sediments share high ammonium concentrations in the range of 2 to at least 6 mM (Fig 2, S1 Table in S1 File). Porewater methane δ^{13}C-CH$_4$ values for Cathedral Hill sediments were generally in the range between -40 and -25 ‰ (VPDB) (S5 Table in S1 File), similar to previously studied methane-rich hydrothermal sediments in Guaymas Basin [14]. Core 4991–35, from cool sediment adjacent to a hydrothermal hot spot (Table 2), differs from hot Cathedral Hill cores by its relatively δ^{13}C-depleted methane (-45 ‰) (S5 Table in S1 File).

The Aceto Balsamico area is located ca. 200 meters south of Cathedral Hill [2]; here, moderately warm sediments are covered with lime-yellow mats of sulfur deposits and sulfur-oxidizing bacteria (Fig 1). The thermal gradient reaches ca. 25 to 30°C at 40 cm depth (Fig 2). The name for this mat area is derived from the near-millimolar porewater acetate concentrations recorded within approximately 30 cm sediment depth, more than an order of magnitude higher than the moderate acetate concentrations (10–20 µM) observed at other mat-covered sediments of Guaymas Basin [2]. Sediments at this location are sulfate-depleted, sulfidic and

Fig 2. Thermal and porewater geochemical profiles of Guaymas Basin sediments. Most porewater samples were obtained by Rhizon sampling, and some ammonium and nitrate data were obtained by centrifugation (cores 4992–22,23 and 4998–13,18). Rhizon-based porewater data are tabulated in S1 Table in S1 File, and centrifugation-based data in S2 and S3 Tables in S1 File.

https://doi.org/10.1371/journal.pone.0256321.g002

rich in ammonia, best illustrated by cores from Dive 4992 (Fig 2), and the sediment-water interface shows local accumulation of elemental sulfur or polysulfides [2]. Porewater methane δ^{13}C-CH$_4$ values for the temperate Aceto Balsamico sediments were generally between -47 and -55 ‰ (VPDB) (S5 Table in S1 File), clearly more depleted in δ^{13}C-CH$_4$ than other hydrothermal sediments in Guaymas Basin [14].

Nearby, the Marker 14 area (named for the site marker placed there in 2009, and still present in 2018) contains hotter sediments where extensive yellow mats transition into localized spots of orange-colored filamentous *Beggiatoaceae* (Fig 1) that are indicative of strong hydrothermal circulation [9]. Hydrothermal sediments from this area have been studied extensively by 16S rRNA gene sequencing and metagenomic analyses to demonstrate that prokaryotic microbial community composition and function are primarily controlled by hydrothermal and geochemical gradients [14, 23]. The Marker 14 sediments were sampled in the anticipation that they provide a geochemical and microbial intermediate between classic Guaymas Basin hydrothermal sediments (orange mats, sulfate inmixing, surficial nitrate peaks, steep temperature gradients) and Aceto Balsamico sediments (yellow precipitates, moderate temperatures, no sulfate inmixing, no nitrate). High ammonium concentrations of 2–10 mM are shared by all three categories of hydrothermal sediment (Fig 2; S1, S3 Tables in S1 File). The δ^{13}C-CH_4 values of Marker 14 sediments (S5 Table in S1 File) matched those of previously studied sediment cores from this area [9, 14]. Interestingly, some thermal gradients at Marker 14 (measured during *Alvin* Dive 4998) were the steepest encountered during the entire expedition and could not be fully recorded as the thermal sensors of the heat flow probe reached their limit (>115˚C) within 30 cm depth (Fig 2). As found previously in Guaymas Basin, hydrothermal activity patterns and thermal gradients are highly localized and vary over short distances [14].

In olive-brown background sediments lacking microbial mats (Fig 1), sulfate persisted at seawater concentrations, sulfide was not detectable, and nitrate remained in the range of a few micromolar to below detection. Ammonium accumulated to only moderate concentrations (160 µM) at depth. The thermal gradient was strongly attenuated (3.2˚C at 5 cm depth, 3.8˚C at 45 cm depth), porewater sulfide was not detectable, and porewater sulfate remained near seawater concentration throughout the core (Fig 2, S1, S3 Tables in S1 File). Strictly speaking, even a thermal gradient of 0.6˚C per 40 cm or 1.5˚C/m is evidence for residual hydrothermal activity that pervades the entire hydrothermal area in the southern spreading center of Guaymas Basin [2]. Therefore, these sediments are "background" only in comparison to more active sites. Interestingly, they contain residual methane with highly δ^{13}C-depleted δ^{13}C-CH_4 values, approximately -65 to -70 ‰ (S5 Table in S1 File), similar to residual methane from cold "background" sediments analyzed previously [14].

Analyses of centrifuged porewater and sediment cakes illustrate the geochemical differences between hydrothermal cores and background, and with sediment depth, on a core-by-core basis (S3 Table in S1 File), and also when multiple cores from particular sampling areas—Cathedral Hill, Aceto Balsamico and Marker 14—are averaged (S4 Table in S1 File). Averaged ammonium concentrations between 2 to 6 millimolar in these hydrothermal cores contrast with 0.12 mM in background sediment (S4 Table in S1 File). Averaged DIC concentrations for cores from Cathedral Hill (62 mg/L), Aceto Balsamico (101 mg/L) and Marker 14 (72 mg/L) exceed those of background sediment (31 mg/L) and cold Cathedral Hill cores (26 mg/L) by factor two or three (S4 Table in S1 File). Porewater DOC and DON concentrations averaged separately for Cathedral Hill (94 and 58 mg/L), Aceto Balsamico (117 and 84 mg/L), and Marker 14 hydrothermal sediments (181 and 107 mg/L) are quite similar to each other (S4 Table in S1 File). In cold background sediment, DOC concentrations remain similar to hydrothermal sediments (90 mg/L), but DON concentrations are almost two orders of magnitude lower (3 mg/L). Two cold cores collected outside of a Cathedral Hill mat (4991–37 and 38) also show a wide difference between DOC (average 39 mM) and DON (average 1.2 mM) porewater concentrations (S4 Table in S1 File). For Cathedral Hill, Aceto Balsamico and Marker 14 hydrothermal sediment, DOC and DON concentrations show contrasting depth trends; DOC decreases with depth whereas DON increases (or shows no visible trend, in Cathedral Hill) (S4 Table in S1 File). In all sampling locations except the background site, TOC and TON content

decrease with sediment depth (S4 Table in S1 File). These trends are consistent with geochemical observations and experimental evidence that hydrothermal activity mobilizes biomass and organic carbon from deeper sediment layers towards the sediment/water interface [5].

Phylum- and class-level community composition

Bacterial and archaeal community composition at the Domain, Phylum and Class levels highlight differences within and between sampling sites (S3-S5 Figs in S1 File). All microbial community analyses in this study have to be qualified by the fact that they are based on sequence frequencies, which are derived from the microbial community but do not necessarily represent it in identical proportions due to potential taxonomic biases in recovery of nucleic acids and amplification of marker genes, as well as variations in gene copy numbers.
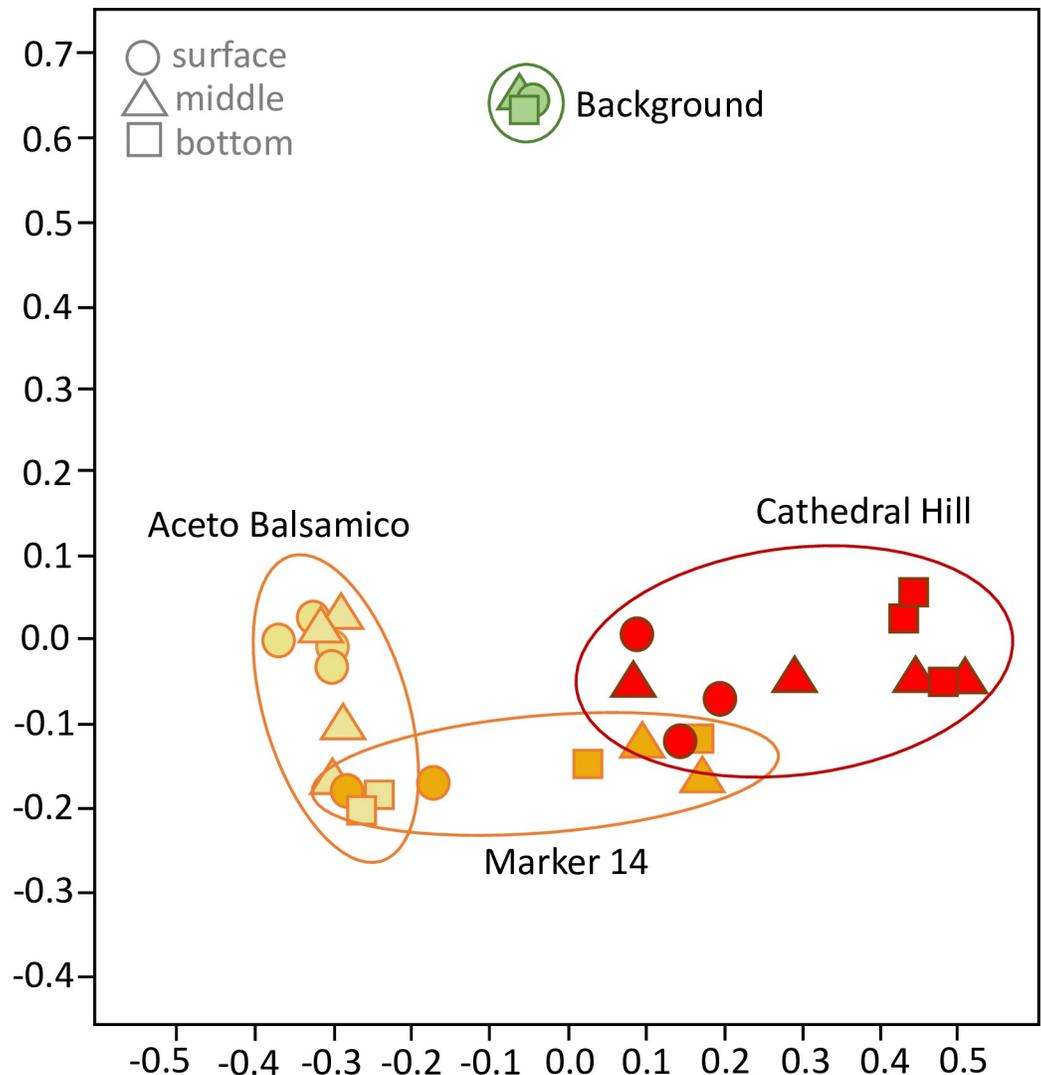
Archaeal signatures increase proportionally with increasing temperature, from approximately 10% in cold background sediment to around 20% in the temperate Aceto Balsamico sites. In the hot Marker 14 and Cathedral Hill sediments, archaeal ASVs increase with depth from 50 to 80% of recovered prokaryotic ASVs (S3 Fig in S1 File). At the phylum- and class-level composition (S4, S5 Figs in S1 File), the Gamma- and Deltaproteobacteria, Planctomycetes and Chloroflexi that predominate in the background sediment yield to predominantly Atribacteria of the JS1 lineage [53], Deltaproteobacteria, and Methanomicrobia in the Aceto Balsamico sediments, with epsilonproteobacterial Campylobacteria as a fourth major group in surficial sediments. At Marker 14 sites, the surficial sediment communities resemble the bacterially dominated Aceto Balsamico community, but the proportions of Bathyarcheota and Thermoplasmata increase downcore. The Cathedral Hill sites show a larger degree of site-specific variability, but harbor presumably thermophilic Acetothermiia [54], consistently in all samples, and show downcore increasing proportions of Thermoplasmata, Crenarchaeota and Bathyarchaeota (S4, S5 Figs in S1 File).

Principal coordinate analyses of bacterial and archaeal communities

Phylogenetic analyses indicate site-specific differences in bacterial and archaeal community composition. To test this possibility more rigorously, Principal Coordinate Analysis was performed on the complete bacterial and archaeal sequence dataset, and indeed this analysis separated the bacterial and archaeal populations according to sample collection area (Fig 3). The tightly clustered Background samples are separated from all other sites. The Aceto Balsamico samples are separated from Cathedral Hill samples, and the Marker 14 samples are connecting these two hydrothermal sample sets. Specifically, Marker 14 shallow (0–10 cm) and deep (10–20 cm) samples are associated with deep (10–20 and 20–30 cm) Aceto Balsamico and shallow (0–10 cm) Cathedral Hill samples, respectively (S6 Fig in S1 File). When the background samples are omitted from the analysis, the Aceto Balsamico and Cathedral Hill samples remain separated, with Marker 14 samples intermediate between them (S7 Fig in S1 File). Notably, site-specific clustering is also observed when the ordination analysis is performed with only Archaea or only Bacteria (S8 Fig in S1 File), indicating that bacterial and archaeal communities follow similar structuring patterns independently. Phylogenetic analyses and balloon plots of methane-cycling archaea (S9 and S10 Figs in S1 File) and sulfate-reducing bacteria (S11 and S12 Figs in S1 File) demonstrate site-specific occurrence patterns also at the level of genus- or family-level lineages (S13 Fig in S1 File, and S1 Text in S1 File).
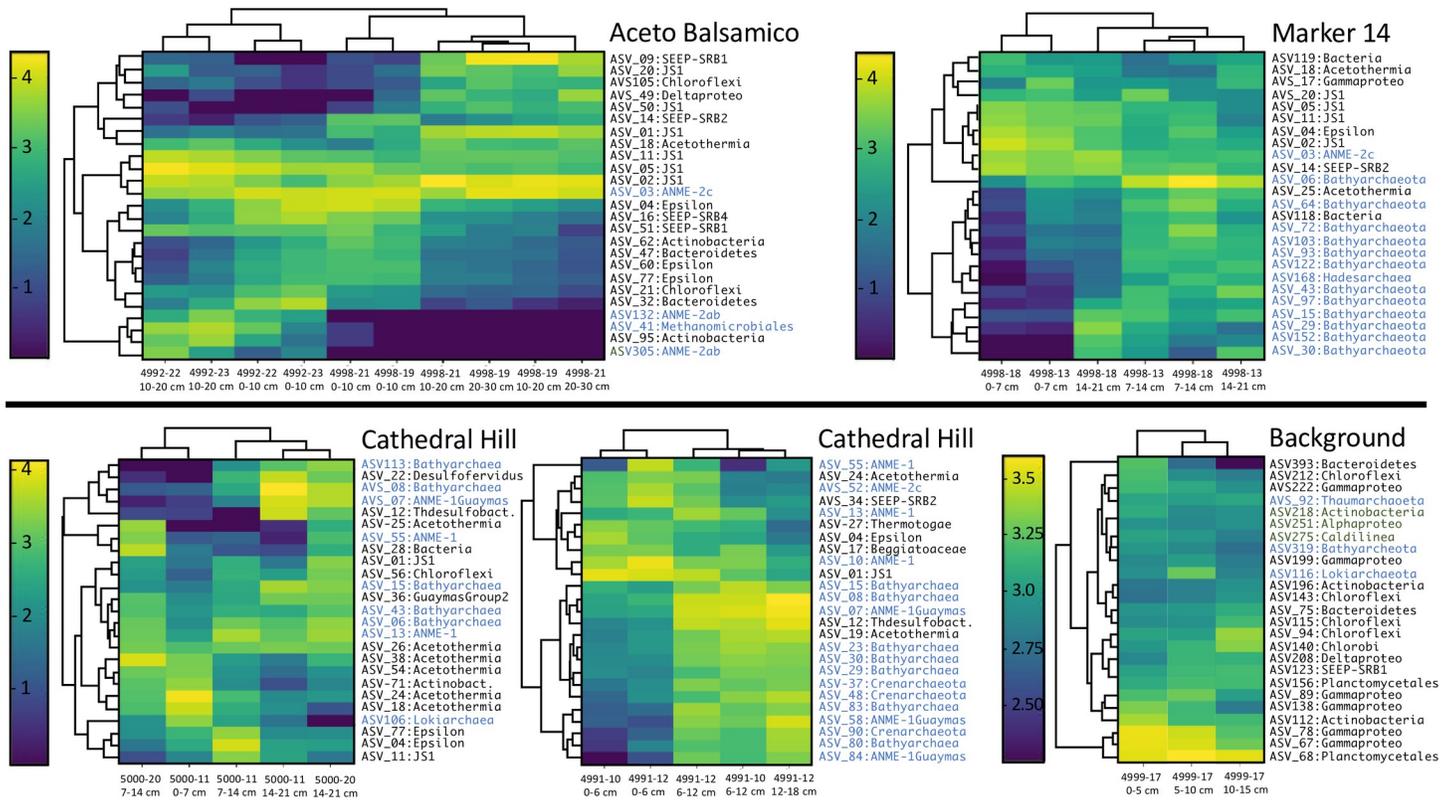
ASV frequency patterns

Adding taxon specificity to phylum- and class-level community patterns, heatmaps of ASV occurrences show site- and depth-specific distribution patterns of the most frequently detected

Fig 3. Cluster analysis of bacterial and archaeal populations. Principal Coordinate Analysis of Bacterial and Archaeal communities in Guaymas Basin sediments, color- and symbol-coded by site (Cathedral Hill, Aceto Balsamico, Marker 14, and Background) and by core position (surface, middle, and bottom sediment). The horizontal and vertical axis account for 23.4% and 17% of the dataset variance, respectively. A fully annotated version with individual sample labels is available as S6 Fig in S1 File.

https://doi.org/10.1371/journal.pone.0256321.g003

bacterial and archaeal ASVs (Fig 4). In the cold background sediment, the 25 most frequently occurring ASVs are primarily assigned to Gamma- and Deltaproteobacteria, Planctomycetes and Chloroflexi; archaeal ASVs are limited to three representatives of the Thaumarchaeota, Bathyarchaeota and Lokiarchaeota (Fig 4). In the temperate Aceto Balsamico cores, epsilon-proteobacterial ASVs appear in the surface sediment and Atribacteria (JS1) ASVs occur throughout all samples. Different deltaproteobacterial ASVs show distinct depth preferences: ASV16 for the surface sediment and ASV09, 14 and 49 for deeper sediments depths (Fig 4). Three of the four archaeal ASVs (ANME-2ab and Methanomicrobiales) appear preferentially in surface layers, and one ASV (ANME-2c) in deeper samples. Similar to Aceto Balsamico, the surface layers at Marker 14 harbor mostly atribacterial ASVs and representatives of the Gamma-, Delta- and Epsilonproteobacteria, but archaeal ASVs (mostly Bathyarchaeota)

Fig 4. Bacterial and archaeal ASV heatmap in Guaymas Basin sediment samples. Scale bars showing log-scale ASV frequencies extend from less frequent ASVs in dark blue to frequent ASVs in lime green. Frequency scales are adjusted to each sampling location. Branching patterns on the left of each heatmap show groupings of ASVs that occur with similar frequency across the sample set; branching patterns on top of each heatmap group sediment samples by shared ASV frequency patterns.

appear prominently below the surface sediment and distinguish the ASV patterns of the deeper, warmer sediments (Fig 4). The consistent depth patterns shown by bacterial and archaeal ASVs in the Aceto Balsamico and Marker 14 sites differ from the core-to-core variability observed in the hot Cathedral Hill sites. Yet, several bathyarchaeotal and ANME-1 ASVs (in cores from *Alvin* dive 5000) and bathyarchaeotal, ANME-1 and Crenarchaeotal ASVs (in cores from *Alvin* dive 4991) show a preference for deeper and warmer sediment layers in Cathedral Hill samples (Fig 4).

Fungal populations

A total of 2,653 fungal intergenic spacer sequences with a mean length of ~400bp were recovered from the Guaymas sediment libraries, and the resulting fungal ASVs affiliated with *Ascomycota* (phylum), *Basidiomycota* (phylum), *Glomeromycota* (phylum), *Chytridiomycota* (phylum), *Kickxellomycota*, (subphylum of Zoopagomycota), *Mortierellomycota* (subphylum of Mucoromycota), *Mucoromycota* (phylum), *Neocallimastigomycota* (phylum), *Rozellomycota* (subphylum of Ophistosporidia, previously named Cryptomycota) and unidentified fungi (Fig 5), based on recently established phylogeny and taxonomy [55]. In fungal ASV frequencies across the sample set, particular taxa are not linked with specific sample areas: *Chytridiomycota* and *Agaricomycetes* were widely distributed across the sample set, whereas *Malasseziomycetes* and *Saccharomycetes* showed relative abundance peaks in individual samples but not linked to a particular sampling area (Fig 5). Approximately one third of fungal iTags from Guaymas sediments remained unclassified, and one quarter of all fungal ASVs belong to "unidentified"

fungi (26%). Unclassified fungal taxa are frequently recovered in different mycobiomes including sediments [56]. These "unidentified" fungal populations are particularly conspicuous in Cathedral Hill samples, where they show locally increased abundance (Fig 5).

Unexpectedly, zoosporic fungi of the *Chytridiomycota* predominate in Guaymas Basin sediments and account for 54% of all fungal ASVs in these sediment samples. Their abundance in Guaymas Basin contrasts with their frequent absence from previously analyzed deep-sea sediments [57, 58], hydrothermal deep-sea sediments [59] and deep bedrock ground water [60]. Only a few studies have detected this basal fungal lineage in deep-sea hydrothermal vents [61], deep-sea sediments [62], and submarine canyons [63], albeit at low proportions compared to other fungal phyla (from 0.8 to 4% of the total reads). As another basal fungal lineage, members of the *Rozellidea* subphylum have been detected in methane cold seeps in relatively high proportion with approximately one third of the total OTUs generated using cloning and sequencing [64]. Here, out of 302 *Chytridiomycota* ASVs recovered from these Guaymas sediments, order-level identifications were limited to 9 ASVs affiliated with the *Rhizophydiales*, and single ASVs assigned to the sister orders *Spizellomycetales* and *Rhizophlyctidales*, whereas the remaining chytridiomycotal ASVs remained taxonomically unresolved.

The *Ascomycota* account for 7% of all fungal ASVs, and fall predominantly into the *Saccharomycetes*, *Dothideomycetes* and *Eurotiomycetes*, which account for 64, 15, and 11.5% of all Ascomycota sequences in the Guaymas samples, respectively. The *Basidiomycota* account for 11% of all fungal ASVs, predominantly *Agaricomycetes* and *Malasseziomycetes* (49 and 30% of *Basidiomycota*, respectively). In some deeper samples, the *Agaricomycetes*, *Malasseziomycetes*, *Saccharomycetes* or fungi of unknown affiliation take the place of the otherwise omnipresent chytrids (Fig 5). Such a pattern contrasts with the frequent dominance of *Ascomycota* and *Basidiomycota* in the marine environment [65, 66], and shows that hydrothermal sediments of the Guaymas Basin represent an untapped reservoir of fungal diversity.

Environmental parameters shaping the fungal community composition

The phylogenetic bubble plot profile (Fig 5) indicates that the fungi do not show taxon-specific preferences for any of the hydrothermal sampling areas or our control site, in stark contrast to the pattern observed for bacteria and archaea (S10 and S12 Figs in S1 File). To examine this observation more rigorously, PCoA analysis was performed on the complete fungal dataset of intergenic spacer sequences. This analysis confirmed the lack of clustering by sampling site (Fig 6, S14 Fig in S1 File), but revealed a contrasting pattern of tightly clustered surficial samples from all sampling sites (background, Aceto Balsamico, Marker 14 and Cathedral Hill) with positive axis 1 values (Fig 6). Negative axis 1 values and the full range of axis 2 contained a broad spread of deeper (and a few shallow) sediment layers from hot hydrothermal Cathedral Hill sites where fungal communities appear to be distinct. This pattern indicates that the fungal communities of hotter hydrothermal subsurface sediments are different from each other and from those of the remaining samples, while the surficial fungal communities of different sampling sites, with potentially a single outlier, are generally similar to each other (Fig 6). Given the dynamic nature of hydrothermal sediments, the changing temperatures and chemical compositions of hydrothermal fluids, and their ephemeral flow paths, it is not surprising that at the very active and dynamic Cathedral Hill site, fungal communities exhibit the highest observed degree of variation (Fig 6).

Complementary analyses of the fungal α-diversity depending on several environmental parameters (site, temperature, sediment depth, type of mats) show that while Shannon indices did not reveal any significant differences, measurements of richness and evenness identified significant differences for temperature and sediment depth (S15 Fig in S1 File). Higher
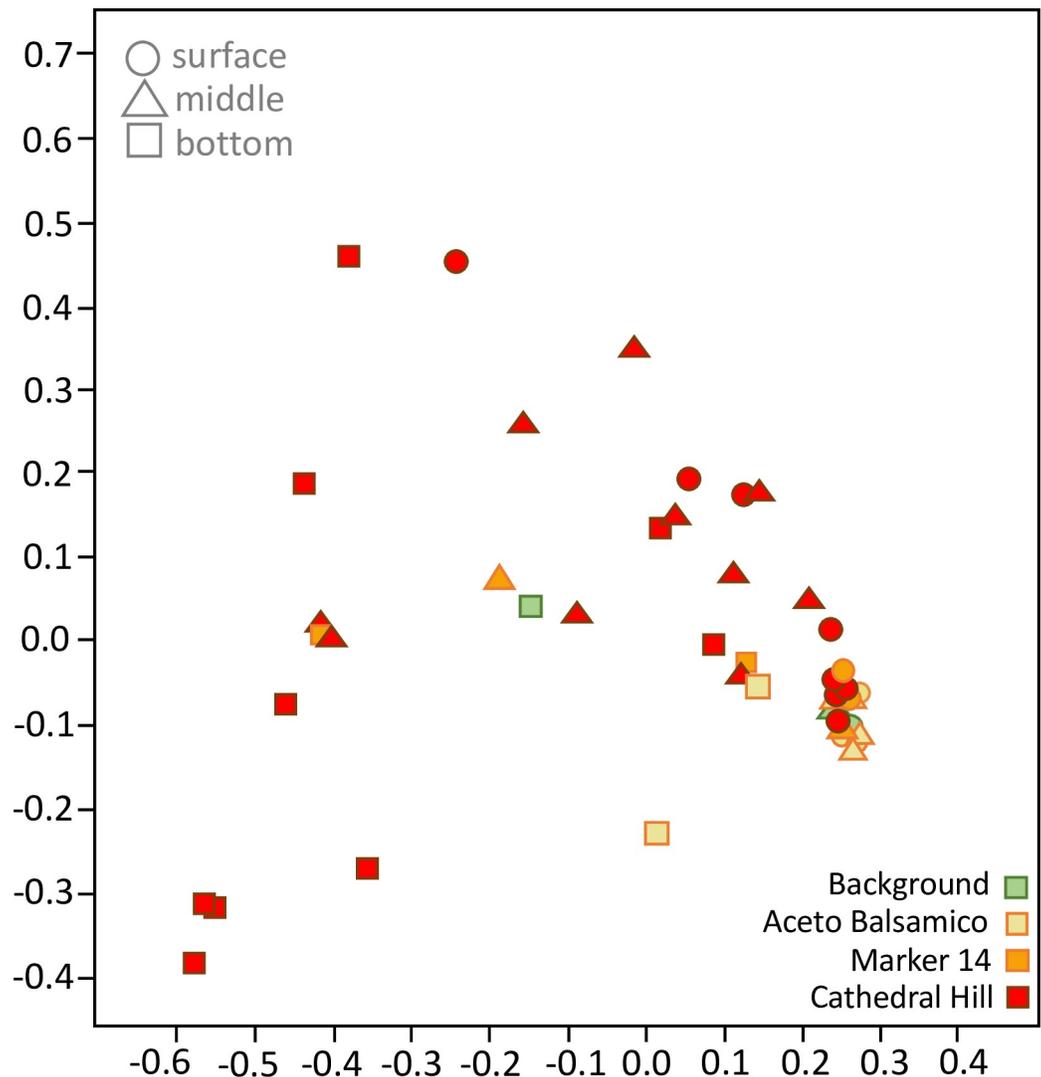
Fig 5. Fungal occurrence patterns in Guaymas sediments. Bubbles are color coded by phylum. Fungal sequences were assigned to class level when possible. Relative phylum abundance is shown in bold. BG stands for background.

richness and lower evenness values were obtained for shallow sediment samples and thus lower temperatures, clearly indicating that a combination of higher fungal diversity and uneven proportions of different fungal taxa characterizes shallow sediment samples.

Co-occurrence network analysis of microbial interactions

In Guaymas Basin, varying environmental and geochemical conditions generate an inherently complex hydrothermal sediment microbiome. To identify microbial interactions within and

Fig 6. Cluster analysis of fungal populations. PCoA analysis of fungal communities based on fungal iTag ASVs in Guaymas Basin samples, color- and symbol-coded by sampling area (Cathedral Hill, Aceto Balsamico, Marker 14, and Background) and by depth (surface, middle, and bottom sediment). The horizontal and vertical axis account for 28.1% and 10.4% of the dataset variance, respectively. A fully annotated version of this figure with individual sample labels is available as S14 Fig in S1 File.
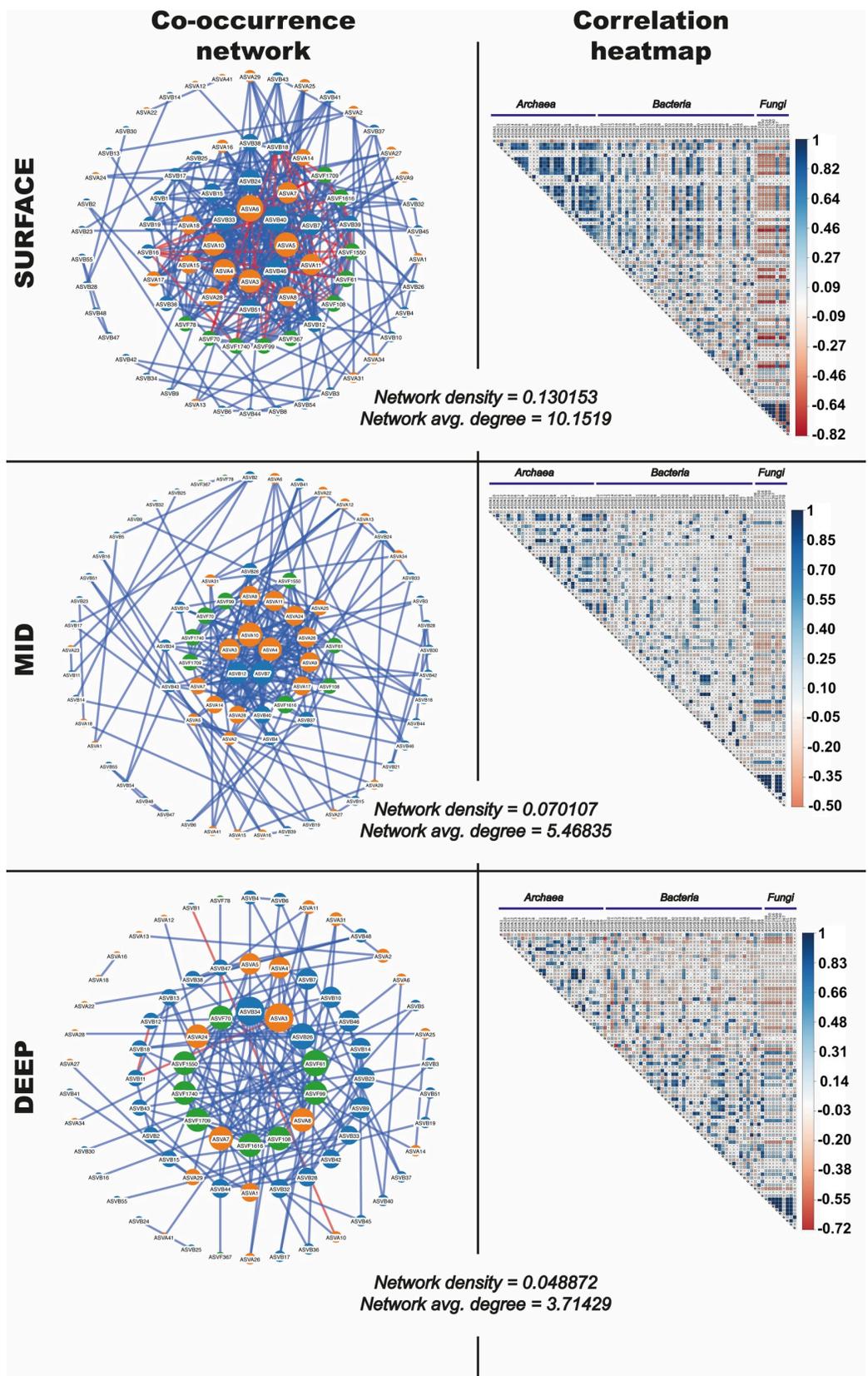
among the archaeal, bacterial and fungal communities in this habitat, the occurrence and abundance profiles of 100 dominant ASVs from these groups were mined for positive and negative ASV-specific co-occurrence interactions (visualized as networks) and correlations (visualized as heatmaps) depending on sample depth (Fig 7) and by sampling sites (Fig 8). With increasing depth, microbial interactions are attenuated, as shown by decreasing network density and average degree values that decrease from 0.130 to 0.049, and from 10.15 to 3.71, respectively. In surface samples, archaeal and bacterial ASVs correlated positively within and between domains, but neither correlated with fungal ASVs (Fig 7). Examination of several network metrics revealed no significant differences for node degree, betweenness and coreness, while eccentricity shows higher values for surface samples compared to intermediate and deep samples (S16 Fig in S1 File). As higher eccentricity assumes higher node proximity, surface ASVs appear more correlated with each other, strongly suggesting more complex interactions between surface ASVs compared to deeper ones.

Different hydrothermal sites strongly re-structure microbial interactions, as revealed by obvious differences in terms of correlations, either positive or negative (Fig 8). While network density and average degree values appear similar between sites, Aceto Balsamico produced a higher number of significant correlations. Specifically, more numerous positive correlations were found between different archaeal ASVs, between archaeal and bacteria ASVs, and within fungal ASVs, but negative correlations dominated between fungal ASVs and bacterial or archaeal ASVs (Fig 8). In the Cathedral Hill hydrothermal samples, the positive correlations between archaeal ASVs and between fungal ASVs persisted, but within a general pattern of increasingly patchy correlations relative to the Aceto Balsamico site (Fig 8). At site Marker 14, a complex patchwork of positive and negative interactions between bacterial and archaeal ASVs erased any domain-based pattern, except for fungal ASVs that remained correlated to each other. Analysis of background samples did not provide any significant correlations. The lower temperatures at Aceto Balsamico, compared to higher temperature ranges at Cathedral Hill and Marker 14, may have favored higher ASV correlations at Aceto Balsamico, and obscured them at the hotter sites. In terms of network metrics (S16 Fig in S1 File), node degree and betweenness did not show site-specific differences, but, generally, higher coreness values were observed for Cathedral Hill and higher eccentricity values were noted for Cathedral Hill and Aceto Balsamico.

Discussion

The bacterial and archaeal communities of Guaymas Basin sediments are highly structured according to site-specific geochemical and thermal conditions, as shown by site-specific PCoA clustering (Fig 3), site-specific ASV distribution patterns (Fig 4), downcore decreasing alpha diversity (S2 Fig in S1 File), downcore increasing archaeal contribution (S4 Fig in S1 File), and site-specific phylum- and class-level changes in microbial community composition (S4, S5 Figs in S1 File). These trends are broadly consistent with observations that phylogenetic profiles and population proportions for bacteria and archaea in Guaymas Basin sediments change along hydrothermal gradients [14, 67], and they complement previous observations of divergent hydrothermal and seep communities in Guaymas Basin and the nearby Sonora Margin [28].

Fungal communities reflect different environmental controls. The dominance of chytrid phylotypes throughout surficial sediment samples (Fig 5) is best explained as a consequence of sedimentary input from the highly productive overlying water column. Chytrids include known phytoplankton parasites, especially of diatoms, chrysophytes and dinoflagellates, and follow the abundance of their hosts [68–71]. Seasonal chytrid blooms in coastal sea ecosystems

Fig 7. Interdomain network correlations in the Guaymas hydrothermal sediments depending on sampling depth.
Nodes represent microbial taxa (orange for archaeal ASVs, blue for bacterial ASVs and green for fungal ASVs) and lines
connect taxa whose abundances were significantly correlated. Nodes are sized depending on degree of interconnectedness.
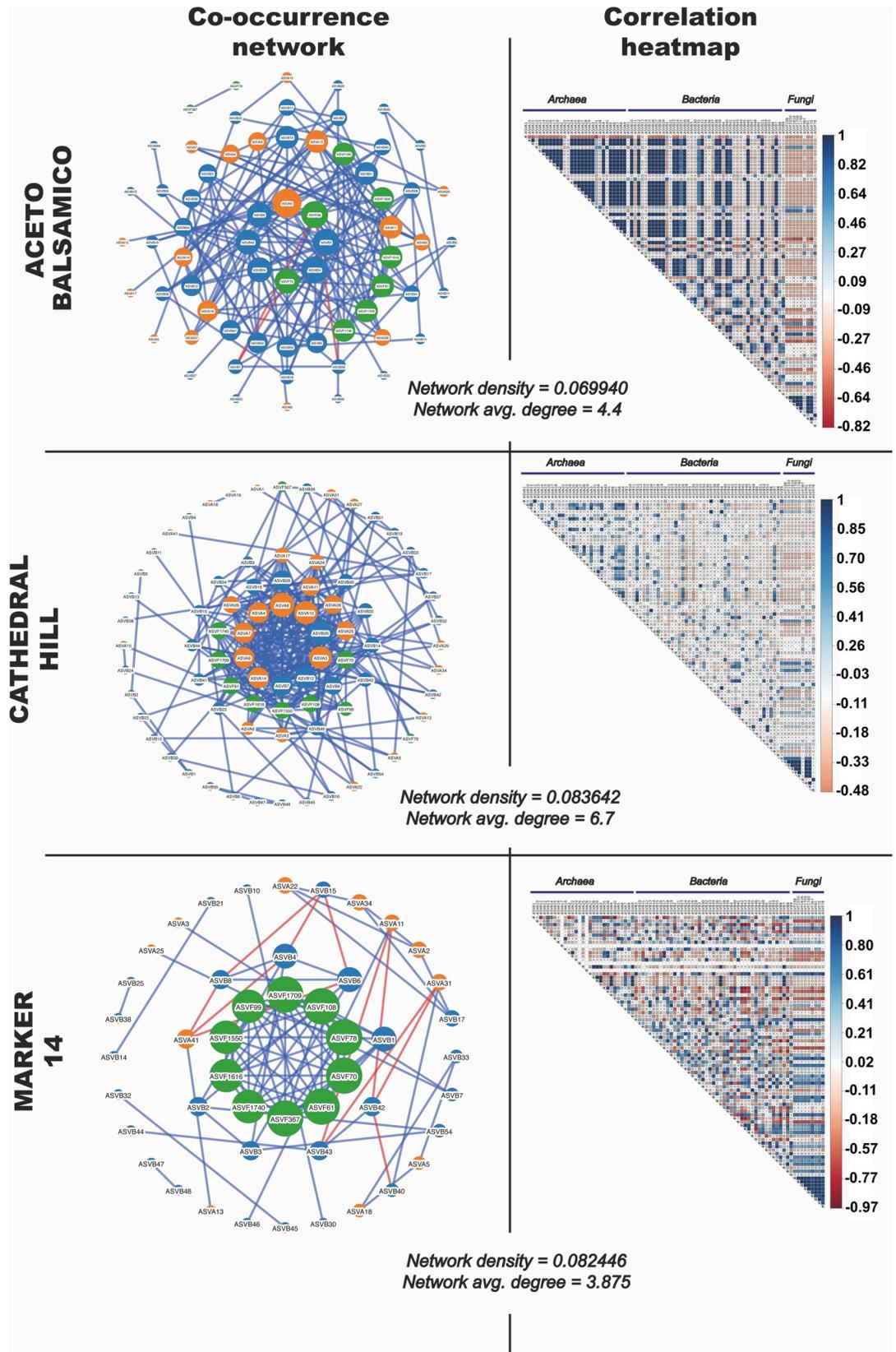Blue lines indicate positive correlations and red lines indicate negative correlations.

corresponded to diatom blooms through multi-year time series analyses [72]. Chytrids are
known to occur in diverse marine habitats [73–76] where their production of motile zoospores
promotes colonization of particulate organic matter such as chitin-rich substrates [77]. In
coastal sediments chytrid occurrence was positively correlated with the presence of dissolved
silicate, an essential nutrient for a diatom-dominated phytoplankton community [78].

Via their parasitic and saprophytic activities, chytrids impact pools and sinking fluxes of
dissolved organic carbon and overall nutrient dynamics in freshwaters, termed the "mycoloop"
[79]. We propose the working hypothesis that the widespread chytrid sequences in Guaymas
Basin sediments are derived primarily from sedimentation of the spring diatom bloom in this
highly productive basin, with terrigenous input as a potential secondary source [80, 81]. After
their arrival on the seafloor, chytrids can sustain themselves by degrading abundant phyto-
plankton biomass [17], and refractory detritus such as chitin [82]. In previous cases where chy-
trids were found at deep-sea hydrothermal sites, interactions with endemic fauna were
suggested [61, 83], but their marked presence in every surficial sediment sample including the
background sediment (Fig 5) indicates that their occurrence in Guaymas Basin is not linked to
hydrothermal conditions or hydrothermal fauna. By contrast, *Saccharomycetes* and *Malassse-
ziomycetes* enrichment below 10 or 20 cm depth (Fig 5) is likely favored by hydrothermal con-
ditions selecting these potentially more thermotolerant taxa over the otherwise omnipresent
chytrids.

In this interpretation, fungal populations in Guaymas Basin surficial sediments arise from
regional sedimentation that ubiquitously imparts a shared chytrid overprint independent of
local hydrothermal conditions. Subsequently, hydrothermal temperatures and steep chemical
gradients emerge as environmental selection factors that become more important downcore,
driving changes in fungal populations in deeper sediment samples. Because our DNA-based
approach detects both viable cells and non-viable extracellular DNA [84], this inference
requires further inquiry using RNA- and culture-based investigations. The taxonomic similar-
ity of surface samples and divergence of deeper samples, respectively, is substantiated by fungal
ordination analysis, where surficial and mid-core samples are tightly clustered, whereas most
deeper sediment samples show a widely scattered pattern (Fig 5). In contrast to bacteria and
archaea, the fungal sequences do not cluster by sampling area (S14 Fig in S1 File). Diversity
indices of the fungal populations reflect the impact of temperature and sediment depth, inde-
pendent of sampling area but linked to sedimentation; chytrid-dominated populations in
cooler, surficial sediments contrast with other fungal populations in deeper, hotter sediments
(S15 Fig in S1 File).

Microbial co-occurrence networks and associated metrics that characterized the hydrother-
mal sediments of Guaymas Basin suggest stronger co-occurrences within domains, and weaker
inter-domain (archaea-bacteria, archaea-fungi and bacteria-fungi) associations. In other
words, representatives of a microbial domain form limited interactions with ASVs from other
domains, but form a cohort with numerous other ASVs within the same domain, i.e. fungal
ASVs were correlated only with other fungal ASVs. These interactions could suggest intra-
domain cooperative metabolisms, and potentially inter-domain competition for resources.
However, this would require further investigation, considering that in environmentally hetero-
geneous ecosystems the dispersal and co-occurrence patterns of microbial communities can be

Fig 8. Interdomain network correlations in the Guaymas hydrothermal sediments depending on sampling site. Nodes represent microbial taxa (orange for archaeal ASVs, blue for bacterial ASVs and green for fungal ASVs) and lines connect taxa whose abundances were significantly correlated. Nodes are sized depending on degree of interconnectedness. Blue lines indicate positive correlations and red lines indicate negative correlations.

jointly driven by deterministic factors, such as specific environmental controls, as well as by stochastic, ecologically neutral processes [85–87].

The absence of correlations between fungal and bacterial/archeal ASVs implies that the fungal community in surficial sediments in Guaymas Basin might not control the structure of functional microbial networks and interactomes, in contrast to what has been described for other habitats [88–90] where co-occurrences between bacteria and fungi resulted from both synergism and antagonism [91], with fungi serving as keystone species that stabilize network properties in complex ecosystems [89, 90]. However, stochastic 'mixing' can mask causal relationships between bacteria and fungi within networks [91]. We hypothesize that the absence of bacterial-fungal co-occurrences in Guaymas Basin sediments may result from such stochastic 'mixing' in this dynamic ecosystem where hydrothermal fluids passing through the thick organic-rich sediments have variable residence times and follow ephemeral pathways [92–94].

While both positive and negative interactions were observed between bacterial and archaeal ASVs close to the sediment surface, these interactions lessened with depth (Fig 7). In contrast, co-occurrences between the most abundant fungal ASVs continued at depth. Fungal co-occurrences exist in complex ecosystems and fungal-fungal interactions are thought to be triggered by largely unknown chemoattractive mechanisms, or by formation of hyphal and mycelial networks [95]. Hyphal and mycelial networks have been described to have ecological "memory" that influences niche partitioning and fungal growth towards new resources [96] while also shaping the plastic behavior that allows fungi to cope with ephemeral resources and competition [97]. Although speculative for Guaymas sediments, the existence of chemoattractive mechanisms and mycelial networks could explain the observed co-occurrences between fungal ASVs at deeper sediment depths.

The absence of inter-domain network interactions involving fungi, and reduced prokaryotic inter-domain network complexity at depth may be linked to harsher environmental conditions downcore that increasingly interfere with microbial interactions. For example, decreasing cell densities downcore due to increasing temperatures may increase the distances between potentially interactive cells and limit the magnitude of interactions. Overall, cross-domain microbial interactions and associations appear to be overwritten by environmental selection factors at Guaymas Basin, whereas other marine [98] or terrestrial [99] habitats show significant cross-domain associations.

Potential selection factors that overwrite microbial interactions and associations in Guaymas Basin include hydrothermal carbon and energy sources. Methane is a dominant carbon species in Guaymas Basin surficial sediments [14] and its availability influences microbial community composition. Stable carbon-isotopic signatures of methane carbon in Cathedral Hill and Marker 14 samples show the isotopic imprint of methane oxidation, as δ^{13}C-CH$_4$ values shift from the hydrothermal baseline of the southern Guaymas Basin vent field (near -42 to 43‰, [14]) towards heavier (less negative) values (S5 Table in S1 File). Consistent with this isotopic evidence for microbial methane oxidation, hydrothermal sediments in the Cathedral Hill and Marker 14 area have high proportions of ANME archaea, especially ANME-1 and ANME-1Guaymas lineages (S10, S13 Figs in S1 File). Interestingly, the light δ^{13}C-CH$_4$ values (near -50 ‰) in the Aceto Balsamico sediments (S5 Table in S1 File) suggest that a contribution of microbial methane in these temperate sites mutes the isotopic consequences of anaerobic methane oxidation. Microbial methane in Guaymas Basin and the nearby Sonora Margin has

δ^{13}C-CH$_4$ values of –70 to –80 ‰ [14, 100], and in this regard resembles the δ^{13}C-CH$_4$ values of trace methane in the background sediment (S5 Table in S1 File). In addition to methane, the availability of hydrothermally produced hydrocarbons influences the microbial community. Several sulfate-reducing lineages within the Deltaproteobacteria (i.e. *Desulfatiglans* lineage, *Desulfobacteraceae* and *Syntrophaceae*) are well-represented, particularly in Marker 14 and Acetobalsamico (S11 and S12 Figs in S1 File), and these lineages specialize in direct or syntrophic oxidation of aromatic and aliphatic hydrocarbons (reviewed in [22]).

The impact of specific carbon substrates on the fungal community is unresolved. Potential carbon sources for fungi in marine sediments that are accessed via exoenzyme secretion include refractory polysaccharides [101] and refractory carbohydrates (e.g., beta-glucans) [102]. Fungi take part in degradation of hydrocarbons in soils and sediments, including aromatic compounds [103–105]. Physiologically versatile fungi persist in the deep subsurface biosphere, and have been cultivated from coal-bearing deep subsurface sediments at 2 km depth [106, 107]. Over 100 fungal genera are known to play important roles in biodegradation [108]. The site-specific hydrothermal fungal communities (with numerous uncharacterized members) might access available substrates in Guaymas Basin, but intergenic spacer sequences do not specifically identify fungi known to utilize hydrocarbons as a primary carbon source. Yet, novel fungi might tap into the rich reservoir of complex petroleum and light-hydrocarbon compounds produced by the thermal alteration of organic matter [109, 110]. This possibility requires future investigation using fungal enrichment cultures and isolates from Guaymas Basin grown on selected combinations of hydrocarbon substrates to elucidate the metabolic potential of taxonomically unresolved fungal populations.

This study directs our attention to zoosporic fungi as a major component of this fungal dark matter, *i.e.* the uncultured and poorly know taxa affiliated to basal fungal lineages such as Rozellidea and Chytridiomycota [55, 111]. In the marine environment, some zoosporic fungi (*Chytridiomycota*, *Blastocladiomycota*) have been described by microscopy and DNA sequencing, but they are infrequently reported, and successful culturing efforts are restricted to a few marine isolates [112]. Sequencing surveys of zoosporic fungi in aquatic habitats have uncovered unexplored biodiversity, and have placed *Chytridiomycota* into "dark matter fungi" [111]. Chytrid orders detected in Guaymas Basin–*Rhizophydiales*, *Rhizophlyctidales* and *Spizellomycetales*–are linked to inputs from particle flux from the upper water column, and sedimentary particles delivered via tectonic and current-driven sediment flows, and riverine inputs. The *Rhizophydiales* are primary organic decomposers and have been reported in marine sediments (Kongsfjorden, Svalbard) of the High Arctic [113], and in ice cores and seafloor sediment samples from the Alaskan coastal Arctic [69]. Novel chytrids of the order *Rhizophydiales* are described as parasites of dinoflagellates and diatoms [68, 70]. The *Rhizophlyctidales* include mainly soil-inhabiting, cellulose-degrading chytrids, isolated from terrestrial ecosystems [114]. The *Spizellomycetales* contain saprophytic chytrids that sometimes grow inside pollen grains buffered against environmental stresses [115]. Abundant *Rhizophlyctidales* and *Spizellomycetales* 18S rRNA gene sequences from high-altitude soils group with environmental sequences from diverse locations, including deep anoxic marine sediments of Cariaco Basin and high-altitude soils [116, 117]. OTUs belonging to *Spizellomycetales* were identified from deep-sea sediments in the Magellan seamounts [118], although members of this group are thought to be mainly of terrestrial origin. Their survival and/or activity in the deep sea remain open questions.

In addition to the chytrids, other zoosporic fungi are present in Guaymas Basin. The *Neocallimastigomycota*, an early-diverging lineage of zoosporic anaerobic fungi that lack mitochondria and contain hydrogenosomes, are represented by eight ASVs; they are primarily associated with the guts of herbivorous mammals and contain an expanded repertoire of
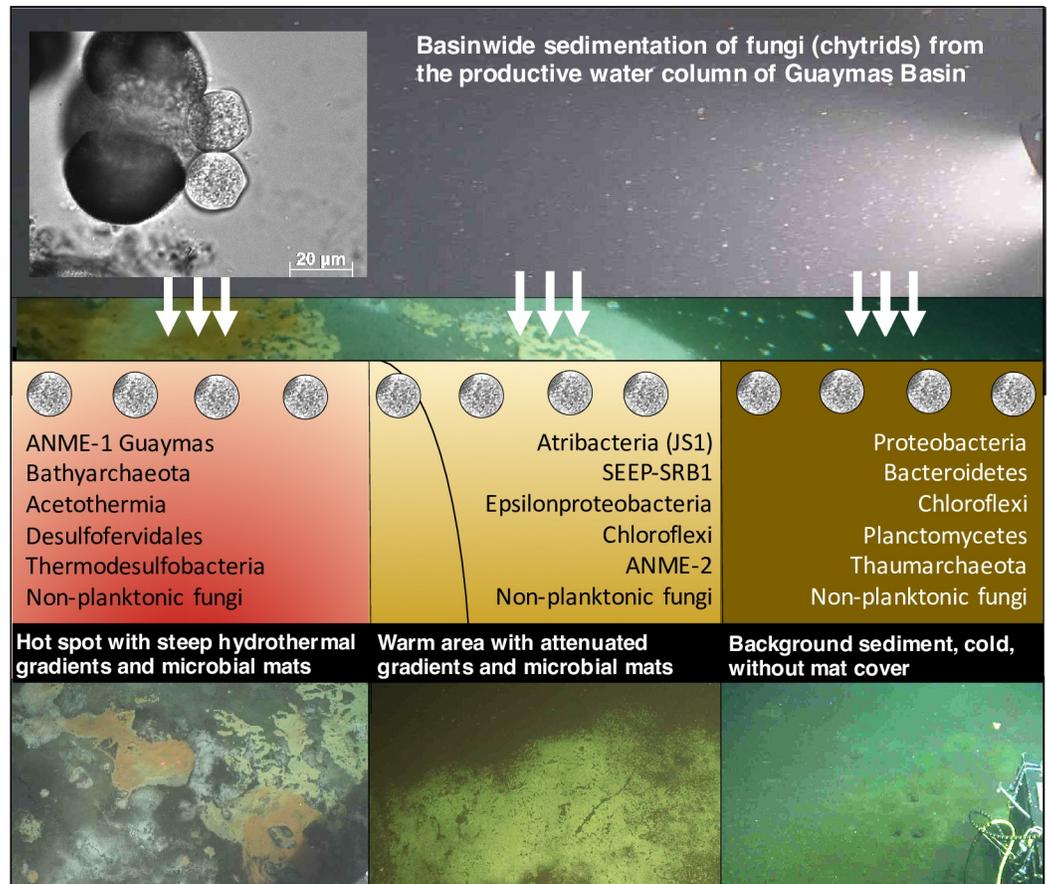
cellulolytic enzymes [55, 119, 120]. The *Neocallimastigomycota* Guaymas ASVs affiliate loosely with *Piromyces* sp. and uncultured *Neocallimastigales*, with the caveat that BLAST alignments show a low percentage identity (~80%) and coverage (~45%). Different *Piromyces* species are able to generate hydrogen, acetate and formate as end-products of a prokaryotic-type mixed-acid fermentation in the rumen of herbivores, e.g. goats [121]. Cultivated *Neocallimastigomycota* isolates so far require growth temperatures of 39°C [121, 122]. The surficial Guaymas sediments that harbor *Neocallimastigomycota* ASVs had a measured temperature range between 3–15°C, however, fermentation of complex carbohydrates to short-chain fatty acids and hydrogen are plausible processes under the biogeochemical regime of Guaymas sediments, and temperatures are known to fluctuate in hydrothermal sediments. Interestingly, fungal hydrogenosome-based metabolism producing H_2 may feed methanogens and other hydrogen-consuming anaerobic archaea in deep subsurface habitats [123, 124], and thus fungi might participate indirectly in methane and hydrogen cycling.

The shift from chytrids towards other fungal communities below the surficial sediment layers could in part be linked to elevated temperatures that range between 30°-50°C in some of the deeper sediments examined here. Both Ascomycota and Basidiomycota include thermotolerant taxa (e.g. *Saccharomycetes* and *Malassseziomycetes*) that are able to grow between 30°C to 45°C [125]. Most of the currently described *Malassezia* yeasts are characterized by their ability to grow at elevated temperatures, such as 45°C [125]. Culture-based and metabarcoding analyses of different substrate types at shallow hydrothermal vents [126], deep-sea hydrothermal sediments [59] and deep-sea hydrothermal vents [83, 127] also reveal *Agaricomycetes*, *Malasseziomycetes*, and *Saccharomycetes* as dominant taxa within fungal communities in those hydrothermal vent ecosystems. Future laboratory studies can reveal the capabilities of diverse chytrids and other zoosporic fungi to grow on diverse carbon sources that are available in Guaymas Basin sediments. These include marine phytoplankton biomass or terrestrial organic matter, as well as diverse hydrocarbons. High-temperature cultivations are likely to yield thermotolerant or even thermophilic fungi among the *Ascomycota* and *Basidiomycota*. The shift towards elevated temperatures deeper in these cores may coincide with changing modes of fungal nutrition and changing substrate preferences, from hydrolysis and fermentation of plankton-derived polymers towards hydrocarbon utilization.

Conclusions

The establishment and structuring of cohabitating prokaryotic and fungal communities in Guaymas Basin surficial sediments respond to fundamentally different environmental cues. For bacteria and archaea, varying thermal and geochemical states dictate site-specific community composition with depth-dependent decreases in community richness, and increases in the relative abundance of archaea. Concentrations of methane and sulfate, temperature, and the presence of aromatic and aliphatic hydrocarbons impact sedimentary microbial communities. In contrast, fungal communities in surficial sediments from different sites are mutually similar, implying a "regional blanketing" of fungi dominated by chytrids (Fig 9). While chytrids persist at all sediment depths sampled at the relatively cool background and temperate sites, the steep thermal gradients at Cathedral Hill result in downcore relative enrichment of both unidentified and known thermotolerant fungal lineages over chytrids.

Several avenues are opening for future fungal research in Guaymas Basin. To determine the likely sources of chytrids and other zoosporic fungi, targeted cultivations should be combined with tests of their ability to grow on marine phytoplankton biomass or terrestrial organic matter. High-temperature cultivations are likely to yield thermotolerant or even thermophilic fungi among the *Ascomycetes* and *Basidiomycetes*, but potentially in other lineages as well.

Fig 9. Conceptual summary. Localized hydrothermal gradients and characteristic microbial populations in Guaymas Basin sediments are superimposed on location-independent biogenic sedimentation from the productive water column, the likely source of ubiquitous chytrid biosignatures in surficial sediments. The insert image at the top left shows chytrids isolated from the estuarine water column of Salt Pond, Falmouth, MA growing on a pollen grain (image courtesy of Edgcomb lab).

https://doi.org/10.1371/journal.pone.0256321.g009

Elevated temperatures may also drive changes in modes of nutrition and substrate spectra, from hydrolysis and fermentation of plankton-derived polymers towards hydrocarbon utilization. Importantly, this study highlights different ecological responses of the prokaryotic and fungal sedimentary community fractions. Understanding how each community responds to site-specific environmental challenges and opportunities will shed light on the nature, extent, and impact of microbial carbon cycling in the diverse hydrothermal environments of Guaymas Basin.

Supporting information

S1 File.
(PDF)

Acknowledgments

Author Contributions

Conceptualization: Samantha B. Joye, Virginia P. Edgcomb, Andreas P. Teske.

Data curation: Andreas P. Teske.

Formal analysis: Gustavo A. Ramírez, Paraskevi Mara, Taylor Sehein, Christopher R. Chambers, Richard N. Peterson, Aurélie Philippe, Gaëtan Burgaud, Andreas P. Teske.

Funding acquisition: Virginia P. Edgcomb, Andreas P. Teske.

Investigation: Gustavo A. Ramírez, Paraskevi Mara, Taylor Sehein, Gunter Wegener, Christopher R. Chambers, Samantha B. Joye, Richard N. Peterson, Aurélie Philippe, Gaëtan Burgaud, Virginia P. Edgcomb, Andreas P. Teske.

Methodology: Gustavo A. Ramírez, Gunter Wegener, Virginia P. Edgcomb, Andreas P. Teske.

Project administration: Virginia P. Edgcomb, Andreas P. Teske.

Resources: Andreas P. Teske.

Software: Gustavo A. Ramírez.

Supervision: Gunter Wegener, Virginia P. Edgcomb, Andreas P. Teske.

Validation: Gustavo A. Ramírez, Andreas P. Teske.

Visualization: Gustavo A. Ramírez.

Writing – original draft: Gustavo A. Ramírez.

Writing – review & editing: Gustavo A. Ramírez, Paraskevi Mara, Andreas P. Teske.

References

1. Teske A, Callaghan AV, LaRowe DE. Biosphere frontiers of subsurface life in the sedimented hydrothermal system of Guaymas Basin. Front Microbiol. 2014; 5:362. https://doi.org/10.3389/fmicb.2014.00362 PMID: 25132832; PubMed Central PMCID: PMC4117188.

2. Teske A, de Beer D, McKay LJ, Tivey MK, Biddle JF, Hoer D, et al. The Guaymas Basin Hiking Guide to Hydrothermal Mounds, Chimneys, and Microbial Mats: Complex Seafloor Expressions of Subsurface Hydrothermal Circulation. Front Microbiol. 2016; 7:75. https://doi.org/10.3389/fmicb.2016.00075 PMID: 26925032; PubMed Central PMCID: PMC4757712.

3. Von Damm KL, Edmond JM, Measures CI, Grant B. Chemistry of submarine hydrothermal solutions at Guaymas Basin, Gulf of California. Geochim Cosmochim Acta. 1985; 49:2221–37.

4. Pearson A, Seewald JS, Eglinton TI. Bacterial incorporation of relict carbon in the hydrothermal environment of Guaymas Basin. Geochimica et Cosmochimica Acta. 2005; 69(23):5477–86. https://doi.org/10.1016/j.gca.2005.07.007

5. Lin YS, Koch BP, Feseker T, Ziervogel K, Goldhammer T, Schmidt F, et al. Near-surface Heating of Young Rift Sediment Causes Mass Production and Discharge of Reactive Dissolved Organic Matter. Sci Rep. 2017; 7:44864. Epub 2017/03/23. https://doi.org/10.1038/srep44864 PMID: 28327661; PubMed Central PMCID: PMC5361187.

6. Teske A. Guaymas Basin, a hydrothermal hydrocarbon seep ecosystem. In: Marine Hydrocarbon Seeps- Microbiology and Biogeochemistry of a Global Marine Habitat (eds. A. Teske A, Carvalho V), Springer. 2020.

7. Jannasch H, Nelson D, Wirsen C. Massive natural occurrence of unusually large bacteria (Beggiatoa spp.) at a hydrothermal deep-sea vent site. Nature. 1989; 342:834–6.

8. Nelson D, Wirsen C, Jannasch H. Characterization of large autotrophic *Beggiatoa* abundant at hydro-thermal vents of the Guaymas Basin. Appl Environ Microbiol. 1989; 55:2909–17. https://doi.org/10.1128/aem.55.11.2909-2917.1989 PMID: 16348053

9. McKay LJ, MacGregor BJ, Biddle JF, Albert DB, Mendlovitz HP, Hoer DR, et al. Spatial heterogeneity and underlying geochemistry of phylogenetically diverse orange and white Beggiatoa mats in Guaymas Basin hydrothermal sediments. Deep Sea Res I. 2012; 67:21–31. https://doi.org/10.1016/j.dsr.2012.04.011

10. MacGregor BJ, Biddle JF, Siebert JR, Staunton E, Hegg EL, Matthysse AG, et al. Why orange Guaymas Basin Beggiatoa spp. are orange: single-filament-genome-enabled identification of an abundant octaheme cytochrome with hydroxylamine oxidase, hydrazine oxidase, and nitrite reductase activities. Appl Environ Microbiol. 2013; 79(4):1183–90. Epub 2012/12/12. https://doi.org/10.1128/AEM.02538-12 PMID: 23220958; PubMed Central PMCID: PMC3568597.

11. MacGregor BJ, Biddle JF, Teske A. Mobile elements in a single-filament orange Guaymas Basin Beggiatoa ("Candidatus Maribeggiatoa") sp. draft genome: evidence for genetic exchange with cyanobacteria. Appl Environ Microbiol. 2013; 79(13):3974–85. Epub 2013/04/23. https://doi.org/10.1128/AEM.03821-12 PMID: 23603674; PubMed Central PMCID: PMC3697557.

12. MacGregor BJ, Biddle JF, Harbort C, Matthysse AG, Teske A. Sulfide oxidation, nitrate respiration, carbon acquisition, and electron transport pathways suggested by the draft genome of a single orange Guaymas Basin Beggiatoa (Cand. Maribeggiatoa) sp. filament. Mar Genomics. 2013; 11:53–65. Epub 2013/09/10. https://doi.org/10.1016/j.margen.2013.08.001 PMID: 24012537.

13. Schutte C, Teske A, MacGregor BJ, Salman-Carvalho V, Lavik G, Hach P, et al. Filamentous giant *Beggiatoaceae* from Guaymas Basin are capable of both denitrification and dissimilatory nitrate reduction to ammonium (DNRA). Appl Environ Microbiol. 2018; 84. https://doi.org/10.1128/AEM.02860-17 PMID: 29802192

14. McKay L, Klokman VW, Mendlovitz HP, LaRowe DE, Hoer DR, Albert D, et al. Thermal and geochemical influences on microbial biogeography in the hydrothermal sediments of Guaymas Basin, Gulf of California. Environ Microbiol Rep. 2016; 8(1):150–61. https://doi.org/10.1111/1758-2229.12365 PMID: 26637109.

15. Dowell F, Cardman Z, Dasarathy S, Kellermann MY, Lipp JS, Ruff SE, et al. Microbial Communities in Methane- and Short Chain Alkane-Rich Hydrothermal Sediments of Guaymas Basin. Front Microbiol. 2016; 7:17. https://doi.org/10.3389/fmicb.2016.00017 PMID: 26858698; PubMed Central PMCID: PMC4731509.

16. Lever MA, Teske AP. Diversity of methane-cycling archaea in hydrothermal sediment investigated by general and group-specific PCR primers. Appl Environ Microbiol. 2015; 81(4):1426–41. Epub 2014/12/21. https://doi.org/10.1128/AEM.03588-14 PMID: 25527539; PubMed Central PMCID: PMC4309701.

17. Teske A, Hinrichs KU, Edgcomb V, de Vera Gomez A, Kysela D, Sylva SP, et al. Microbial Diversity of Hydrothermal Sediments in the Guaymas Basin: Evidence for Anaerobic Methanotrophic Communities. Appl Environ Microbiol. 2002; 68(4):1994–2007. https://doi.org/10.1128/AEM.68.4.1994-2007.2002 PMID: 11916723

18. Biddle JF, Cardman Z, Mendlovitz H, Albert DB, Lloyd KG, Boetius A, et al. Anaerobic oxidation of methane at different temperature regimes in Guaymas Basin hydrothermal sediments. ISME J. 2012; 6(5):1018–31. https://doi.org/10.1038/ismej.2011.164 PMID: 22094346; PubMed Central PMCID: PMC3329104.

19. Laso-Pérez R, Wegener G, Knittel K, Widdel F, Harding KJ, Krukenberg V, et al. Thermophilic archaea activate butane via alkyl-coenzyme M formation. Nature. 2016; 539(7629):396–401. https://doi.org/10.1038/nature20152 PMID: 27749816.

20. Seitz KW, Dombrowski N, Eme L, Spang A, Lombard J, Sieber JR, et al. Asgard archaea capable of anaerobic hydrocarbon cycling. Nat Commun. 2019; 10(1):1822. https://doi.org/10.1038/s41467-019-09364-x PMID: 31015394; PubMed Central PMCID: PMC6478937.

21. Hahn C, Laso-Pérez R, Vulcano F, Vaziourakis K, Stokke R, Steen IH, et al. "*Candidatus* Ethanoperedens," a Thermophilic Genus of *Archaea* Mediating the Anaerobic Oxidation of Ethane. MBio. 2021; 11:e00600–20. https://journals.asm.org/doi/10.1128/mBio.00600-20.

22. Teske A. Hydrocarbon-degrading anaerobic microbial communities in natural oil seeps. In: McGenity T. J.(ed.), Microbial Communities Utilizing Hydrocarbons and Lipids: Members, Metagenomics and Ecophysiology, Handbook of Hydrocarbon and Lipid Microbiology. Springer, Cham. 2019. https://doi.org/10.1007/978-3-319-60063-5_3-2.

23. Dombrowski N, Teske A, Baker BJ. Exapnsive microbial metabolic versatility and biodiversity in dynamic Guaymas Basin hydrothermal sediments. Nature Comm. 2018; 9(4999):4999. https://doi.org/10.1038/s41467-018-07418-0 PMID: 30479325

24. Dombrowski N, Seitz KW, Teske AP, Baker BJ. Genomic insights into potential interdependencies in microbial hydrocarbon and nutrient cycling in hydrothermal sediments. Microbiome. 2017; 5(1):106. Epub 2017/08/25. https://doi.org/10.1186/s40168-017-0322-2 PMID: 28835260; PubMed Central PMCID: PMC5569505.

25. Edgcomb VP, Kysela DT, Teske A, de Vera Gomez A, Sogin ML. Benthic eukaryotic diversity in the Guaymas Basin hydrothermal vent environment. Proc Natl Acad Sci U S A. 2002; 99(11):7658–62. Epub 2002/05/29. https://doi.org/10.1073/pnas.062186399 PMID: 12032339; PubMed Central PMCID: PMC124314.

26. Bass D, Howe A, Brown N, Barton H, Demidova M, Michelle H, et al. Yeast forms dominate fungal diversity in the deep oceans. Proc Biol Sci. 2007; 274(1629):3069–77. Epub 2007/10/18. https://doi.org/10.1098/rspb.2007.1067 PMID: 17939990; PubMed Central PMCID: PMC2293941.

27. Keeler E, Burgaud G, Teske A, Beaudoin D, Mehiri M, Dayras M, et al. Deep-sea hydrothermal vent sediments reveal diverse fungi with antibacterial activities. FEMS Microbiol Ecol. 2021; 97(8). https://doi.org/10.1093/femsec/fiab103 PMID: 34245561

28. Cruaud P, Vigneron A, Pignet P, Caprais J-C, Lesongeur F, Toffin L, et al. Comparative study of Guaymas basin microbiomes: cold seeps vs. hydrothermal vents sediments. Front Mar Sci. 2017; 4:417. https://doi.org/10.3389/fmars.2017.00417

29. Ramírez GA, McKay LJ, Fields MW, Buckley A, Mortera C, Hensen C, et al. The Guaymas Basin subseafloor sedimentary archaeome reflects complex environmental histories. iScience. 2020; 23 (101459). https://doi.org/10.1016/j.isci.2020.101459 PMID: 32861995

30. Teske A, Wegener G, Chanton JP, White D, MacGregor B, Hoer D, et al. Microbial Communities Under Distinct Thermal and Geochemical Regimes in Axial and Off-Axis Sediments of Guaymas Basin. Front Microbiol. 2021; 12:633649. Epub 2021/03/02. https://doi.org/10.3389/fmicb.2021.633649 PMID: 33643265; PubMed Central PMCID: PMC7906980.

31. Seeberg-Elverfeldt J, Schlüter M, Feseker T, Kölling M. Rhizon sampling of porewaters near the sediment-water interface of aquatic systems. Limnol Oceanogr: Methods. 2005; 3:361–71.

32. Cline J. Spectrophotometric determination of hydrogen sulfide in natural waters. Limnol Oceanogr. 1969; 14:454–8.

33. Grasshoff K, Kremling K, Ehrhardt M. Methods of seawater analysis. John Wiley & Sons. 2009.

34. Wegener G, van Erk M, Teske A. Concentrations of dissolved anions in porewater and gaseous alkanes in sediments retrieved from the Guaymas Basin hydrothermal sediments in 2018. PANGAEA. 2021. https://doi.pangaea.de/10.1594/PANGAEA.931866.

35. Ramírez GA, Graham D, D'Hondt S. Influence of commercial DNA extraction kit choice on prokaryotic community metrics in marine sediment. Limnology and Oceanography: Methods. 2018; 16(9):525–36. https://doi.org/10.1002/lom3.10264

36. Parada AE, Needham DM, Fuhrman JA. Every base matters: assessing small subunit rRNA primers for marine microbiomes with mock communities, time series and global field samples. Environmental Microbiology. 2016; 18(5):1403–14. https://doi.org/10.1111/1462-2920.13023 PMID: 26271760

37. Taylor DL, Walters WA, Lennon NJ, Bochicchio J, Krohn A, Caporaso JG, et al. Accurate Estimation of Fungal Diversity and Abundance through Improved Lineage-Specific Primers Optimized for Illumina Amplicon Sequencing. Appl Environ Microbiol. 2016; 82(24):7217–26. Epub 2016/11/01. https://doi.org/10.1128/AEM.02576-16 PMID: 27736792; PubMed Central PMCID: PMC5118932.

38. Callahan BJ, McMurdie PJ, Rosen MJ, Han AW, Johnson AJ, Holmes SP. DADA2: High-resolution sample inference from Illumina amplicon data. Nat Methods. 2016; 13(7):581–3. Epub 2016/05/24. https://doi.org/10.1038/nmeth.3869 PMID: 27214047; PubMed Central PMCID: PMC4927377.

39. Quast C, Pruesse E, Yilmaz P, Gerken J, Schweer T, Yarza P, et al. The SILVA ribosomal RNA gene database project: improved data processing and web-based tools. Nucleic Acids Res. 2013; 41(Database issue):D590–6. https://doi.org/10.1093/nar/gks1219 PMID: 23193283; PubMed Central PMCID: PMC3531112.

40. Bolyen E, Rideout JR, Dillon MR, Bokulich NA, Abnet CC, Al-Ghalith GA, et al. Reproducible, interactive, scalable and extensible microbiome data science using QIIME 2. Nat Biotechnol. 2019; 37 (8):852–7. Epub 2019/07/26. https://doi.org/10.1038/s41587-019-0209-9 PMID: 31341288; PubMed Central PMCID: PMC7015180.

41. UNITE-Community. UNITE QIIME Release for Fungi. Version 18.11.2018. Available online at: https://forum.qiime2.org/t/unite-v-8-0-2018-11-18-classifiers-for-qiime2-available-here/8750. 2019.

42. McMurdie PJ, Holmes S. phyloseq: an R package for reproducible interactive analysis and graphics of microbiome census data. PLoS One. 2013; 8(4):e61217. https://doi.org/10.1371/journal.pone.0061217 PMID: 23630581; PubMed Central PMCID: PMC3632530.

43. Oksanen J, Blanchet FG, Kindt R, Legendre P, Minchin PR, O'Hara RB, et al. vegan: Community Ecology Package. R Package Version 2.2–1. Available online at: http://CRANR-projectorg/package=vegan. 2015.

44. Venables W, Ripley B. Modern Applied Statistics with S. Fourth Edition. Springer, New York. 2002.

45. Waite DW, Vanwonterghem I, Rinke C, Parks DH, Zhang Y, Takai K, et al. Comparative Genomic Analysis of the Class Epsilonproteobacteria and Proposed Reclassification to Epsilonbacteraeota (phyl. nov.). Front Microbiol. 2017; 8:682. Epub 2017/05/10. https://doi.org/10.3389/fmicb.2017.00682 PMID: 28484436; PubMed Central PMCID: PMC5401914.

46. Waite DW, Chuvochina M, Pelikan C, Parks DH, Yilmaz P, Wagner M, et al. Proposal to reclassify the proteobacterial classes Deltaproteobacteria and Oligoflexia, and the phylum Thermodesulfobacteria into four phyla reflecting major functional capabilities. Int J Syst Evol Microbiol. 2020; 70(11):5972–6016. Epub 2020/11/06. https://doi.org/10.1099/ijsem.0.004213 PMID: 33151140.

47. Zhou Z, Pan J, Wang F, Gu JD, Li M. Bathyarchaeota: globally distributed metabolic generalists in anoxic environments. FEMS Microbiol Rev. 2018; 42(5):639–55. Epub 2018/05/24. https://doi.org/10.1093/femsre/fuy023 PMID: 29790926.

48. Baker BJ, De Anda V, Seitz KW, Dombrowski N, Santoro AE, Lloyd KG. Diversity, ecology and evolution of Archaea. Nat Microbiol. 2020; 5(7):887–900. Epub 2020/05/06. https://doi.org/10.1038/s41564-020-0715-z PMID: 32367054.

49. Murray AE, Freudenstein J, Gribaldo S, Hatzenpichler R, Hugenholtz P, Kampfer P, et al. Roadmap for naming uncultivated Archaea and Bacteria. Nat Microbiol. 2020; 5(8):987–94. Epub 2020/06/10. https://doi.org/10.1038/s41564-020-0733-x PMID: 32514073; PubMed Central PMCID: PMC7381421.

50. Zakrzewski M, Proietti C, Ellis JJ, Hasan S, Brion MJ, Berger B, et al. Calypso: a user-friendly web-server for mining and visualizing microbiome-environment interactions. Bioinformatics. 2017; 33 (5):782–3. Epub 2016/12/28. https://doi.org/10.1093/bioinformatics/btw725 PMID: 28025202; PubMed Central PMCID: PMC5408814.

51. Nagpal S, Singh R, Yadav D, Mande SS. MetagenoNets: comprehensive inference and meta-insights for microbial correlation networks. Nucleic Acids Res. 2020; 48(W1):W572–9. Epub 2020/04/28. https://doi.org/10.1093/nar/gkaa254 PMID: 32338757; PubMed Central PMCID: PMC7319469.

52. Schwager E, Weingart G, Bielski C, Huttenhower C. CCREPE: Compositionality corrected by Permutation and Renormalization. http://www.bioconductor.org/packages/devel/bioc/manuals/ccrepe/man/ccrepe.pdf. 2018.

53. Nobu MK, Dodsworth JA, Murugapiran SK, Rinke C, Gies EA, Webster G, et al. Phylogeny and physiology of candidate phylum 'Atribacteria' (OP9/JS1) inferred from cultivation-independent genomics. ISME J. 2016; 10(2):273–86. Epub 2015/06/20. https://doi.org/10.1038/ismej.2015.97 PMID: 26090992; PubMed Central PMCID: PMC4737943.

54. Takami H, Noguchi H, Takaki Y, Uchiyama I, Toyoda A, Nishi S, et al. A deeply branching thermophilic bacterium with an ancient acetyl-CoA pathway dominates a subsurface ecosystem. PLoS One. 2012; 7(1):e30559. Epub 2012/02/04. https://doi.org/10.1371/journal.pone.0030559 PMID: 22303444; PubMed Central PMCID: PMC3267732.

55. Naranjo-Ortiz MA, Gabaldón T. Fungal evolution: diversity, taxonomy and phylogeny of the Fungi. Biol Rev Camb Philos Soc. 2019; 94(6):2101–37. Epub 2019/10/30. https://doi.org/10.1111/brv.12550 PMID: 31659870; PubMed Central PMCID: PMC6899921.

56. Tedersoo L, Anslan S, Bahram M, Kõljalg U, Abarenkov K. Identifying the 'unidentified' fungi: a global-scale long-read third-generation sequencing approach. Fungal Diversity. 2020; 103(1):273–93. https://doi.org/10.1007/s13225-020-00456-4

57. Singh P, Raghukumar C, Verma P, Shouche Y. Assessment of fungal diversity in deep-sea sediments by multiple primer approach. World J Microbiol Biotechnol. 2012; 28(2):659–67. Epub 2012/07/19. https://doi.org/10.1007/s11274-011-0859-3 PMID: 22806861.

58. Nagano Y, Nagahama T, Hatada Y, Nunoura T, Takami H, Miyazaki J, et al. Fungal diversity in deep-sea sediments–the presence of novel fungal groups. Fungal Ecology. 2010; 3(4):316–25. https://doi.org/10.1016/j.funeco.2010.01.002

59. Xu W, Gong L-f, Pang K-L, Luo Z-H. Fungal diversity in deep-sea sediments of a hydrothermal vent system in the Southwest Indian Ridge. Deep Sea Research Part I: Oceanographic Research Papers. 2018; 131:16–26. https://doi.org/10.1016/j.dsr.2017.11.001

60. Sohlberg E, Bomberg M, Miettinen H, Nyyssonen M, Salavirta H, Vikman M, et al. Revealing the unexplored fungal communities in deep groundwater of crystalline bedrock fracture zones in Olkiluoto, Finland. Front Microbiol. 2015; 6:573. Epub 2015/06/25. https://doi.org/10.3389/fmicb.2015.00573 PMID: 26106376; PubMed Central PMCID: PMC4460562.

61. Le Calvez T, Burgaud G, Mahe S, Barbier G, Vandenkoornhuyse P. Fungal diversity in deep-sea hydrothermal ecosystems. Appl Environ Microbiol. 2009; 75(20):6415–21. Epub 2009/07/28. https://doi.org/10.1128/AEM.00653-09 PMID: 19633124; PubMed Central PMCID: PMC2765129.

62. Zhang X-Y, Wang G-H, Xu X-Y, Nong X-H, Wang J, Amin M, et al. Exploring fungal diversity in deep-sea sediments from Okinawa Trough using high-throughput Illumina sequencing. Deep Sea Research Part I: Oceanographic Research Papers. 2016; 116:99–105. https://doi.org/10.1016/j.dsr.2016.08.004

63. Barone G, Rastelli E, Corinaldesi C, Tangherlini M, Danovaro R, Dell'Anno A. Benthic deep-sea fungi in submarine canyons of the Mediterranean Sea. Progress in Oceanography. 2018; 168:57–64. https://doi.org/10.1016/j.pocean.2018.09.011

64. Nagahama T, Takahashi E, Nagano Y, Abdel-Wahab MA, Miyazaki M. Molecular evidence that deep-branching fungi are major fungal components in deep-sea methane cold-seep sediments. Environ Microbiol. 2011; 13(8):2359–70. Epub 2011/05/25. https://doi.org/10.1111/j.1462-2920.2011.02507.x PMID: 21605311.

65. Jones EBG, Suetrong S, Sakayaroj J, Bahkali AH, Abdel-Wahab MA, Boekhout T, et al. Classification of marine Ascomycota, Basidiomycota, Blastocladiomycota and Chytridiomycota. Fungal Diversity. 2015; 73(1):1–72. https://doi.org/10.1007/s13225-015-0339-4

66. Pang K-L, Jones EBG. Recent advances in marine mycology. Botanica Marina. 2017; 60(4). https://doi.org/10.1515/bot-2017-0048

67. Engelen B, Nguyen T, Heyerhoff B, Kalenborn S, Sydow K, Tabai H, et al. Microbial Communities of Hydrothermal Guaymas Basin Surficial Sediment Profiled at 2 Millimeter-Scale Resolution. Front Microbiol. 2021; 12:710881. Epub 2021/08/03. https://doi.org/10.3389/fmicb.2021.710881 PMID: 34335545; PubMed Central PMCID: PMC8322767.

68. Lepelletier F, Karpov SA, Alacid E, Le Panse S, Bigeard E, Garces E, et al. Dinomyces arenysensis gen. et sp. nov. (Rhizophydiales, Dinomycetaceae fam. nov.), a chytrid infecting marine dinoflagellates. Protist. 2014; 165(2):230–44. Epub 2014/04/09. https://doi.org/10.1016/j.protis.2014.02.004 PMID: 24709472.

69. Hassett B, Gradinger R. Chytrids dominate arctic marine fungal communities Environ Microbiol. 2016; 18:2001–9. https://doi.org/10.1111/1462-2920.13216 PMID: 26754171

70. Garvetto A, Badis Y, Perrineau MM, Rad-Menendez C, Bresnan E, Gachon CMM. Chytrid infecting the bloom-forming marine diatom Skeletonema sp.: Morphology, phylogeny and distribution of a novel species within the Rhizophydiales. Fungal Biol. 2019; 123(6):471–80. Epub 2019/05/28. https://doi.org/10.1016/j.funbio.2019.04.004 PMID: 31126424.

71. Kilias ES, Junges L, Supraha L, Leonard G, Metfies K, Richards TA. Chytrid fungi distribution and co-occurrence with diatoms correlate with sea ice melt in the Arctic Ocean. Commun Biol. 2020; 3(1):183. Epub 2020/04/23. https://doi.org/10.1038/s42003-020-0891-7 PMID: 32317738; PubMed Central PMCID: PMC7174370.

72. Taylor JD, Cunliffe M. Multi-year assessment of coastal planktonic fungi reveals environmental drivers of diversity and abundance. ISME J. 2016; 10(9):2118–28. Epub 2016/03/05. https://doi.org/10.1038/ismej.2016.24 PMID: 26943623; PubMed Central PMCID: PMC4989315.

73. Hassett BT, Ducluzeau AL, Collins RE, Gradinger R. Spatial distribution of aquatic marine fungi across the western Arctic and sub-arctic. Environ Microbiol. 2017; 19(2):475–84. Epub 2016/05/22. https://doi.org/10.1111/1462-2920.13371 PMID: 27207498.

74. Hassett BT, Gradinger R. New Species of Saprobic Labyrinthulea (= Labyrinthulomycota) and the Erection of a gen. nov. to Resolve Molecular Polyphyly within the Aplanochytrids. J Eukaryot Microbiol. 2018; 65(4):475–83. Epub 2017/12/22. https://doi.org/10.1111/jeu.12494 PMID: 29265676.

75. Li W, Wang MM, Wang XG, Cheng XL, Guo JJ, Bian XM, et al. Fungal communities in sediments of subtropical Chinese seas as estimated by DNA metabarcoding. Sci Rep. 2016; 6:26528. Epub 2016/05/21. https://doi.org/10.1038/srep26528 PMID: 27198490; PubMed Central PMCID: PMC4873734.

76. Raghukumar S. Marine microbial eukaryotic diversity, with particular reference to fungi: Lessons from prokaryotes. Indian J Mar Sci. 2006; 35:388–98.

77. Roberts C, Allen R, Bird KE, Cunliffe M. Chytrid fungi shape bacterial communities on model particulate organic matter. Biol Lett. 2020; 16(9):20200368. Epub 2020/09/30. https://doi.org/10.1098/rsbl.2020.0368 PMID: 32991826; PubMed Central PMCID: PMC7532721.

78. Guo X, Zhang Q, Zhang X, Zhang J, Gong J. Marine fungal communities in water and surface sediment of a sea cucumber farming system: habitat-differentiated distribution and nutrients driving succession. Fungal Ecology. 2015; 14:87–98. https://doi.org/10.1016/j.funeco.2014.12.001

79. Kagami M, Miki T, Takimoto G. Mycoloop: chytrids in aquatic food webs. Front Microbiol. 2014; 5:166. Epub 2014/05/06. https://doi.org/10.3389/fmicb.2014.00166 PMID: 24795703; PubMed Central PMCID: PMC4001071.

80. Calvert SE. Origin of diatom-rich, varved sedimetns from the Gulf of California. J Geology. 1966; 74 (5):546–65. https://www.jstor.org/stable/30059298.

81. Calvert SE. "Factors affecting distribution of laminated diatomaceous sediments in the Gulf of California" In Marine Geology of the Gulf of California, Vol. 3, eds. van Andel T.H. and Shor G.G., (Tulsa: American Association of Petroleum Geologists Memorir). 1964; 3:311–30.

82. Gleason FH, Kagami M, Lefevre E, Sime-Ngando T. The ecology of chytrids in aquatic ecosystems: roles in food web dynamics. Fungal Biology Reviews. 2008; 22(1):17–25. https://doi.org/10.1016/j.fbr.2008.02.001

83. Burgaud G, Arzur D, Durand L, Cambon-Bonavita MA, Barbier G. Marine culturable yeasts in deep-sea hydrothermal vents: species richness and association with fauna. FEMS Microbiol Ecol. 2010; 73 (1):121–33. Epub 2010/05/12. https://doi.org/10.1111/j.1574-6941.2010.00881.x PMID: 20455940.

84. Ramírez GA, Jørgensen SL, Zhao R, D'Hondt S. Minimal Influence of Extracellular DNA on Molecular Surveys of Marine Sedimentary Communities. Front Microbiol. 2018; 9:2969. https://doi.org/10.3389/fmicb.2018.02969 PMID: 30564217; PubMed Central PMCID: PMC6288230.

85. Dumbrell AJ, Nelson M, Helgason T, Dytham C, Fitter AH. Relative roles of niche and neutral processes in structuring a soil microbial community. ISME J. 2010; 4(3):337–45. Epub 2009/11/20. https://doi.org/10.1038/ismej.2009.122 PMID: 19924158.

86. Caruso T, Chan Y, Lacap DC, Lau MC, McKay CP, Pointing SB. Stochastic and deterministic processes interact in the assembly of desert microbial communities on a global scale. ISME J. 2011; 5 (9):1406–13. Epub 2011/03/04. https://doi.org/10.1038/ismej.2011.21 PMID: 21368908; PubMed Central PMCID: PMC3160679.

87. Stegen JC, Lin X, Konopka AE, Fredrickson JK. Stochastic and deterministic assembly processes in subsurface microbial communities. ISME J. 2012; 6(9):1653–64. Epub 2012/03/30. https://doi.org/10.1038/ismej.2012.22 PMID: 22456445; PubMed Central PMCID: PMC3498916.

88. de Menezes AB, Prendergast-Miller MT, Richardson AE, Toscas P, Farrell M, Macdonald LM, et al. Network analysis reveals that bacteria and fungi form modules that correlate independently with soil parameters. Environ Microbiol. 2015; 17(8):2677–89. Epub 2014/07/22. https://doi.org/10.1111/1462-2920.12559 PMID: 25040229.

89. Tipton L, Muller CL, Kurtz ZD, Huang L, Kleerup E, Morris A, et al. Fungi stabilize connectivity in the lung and skin microbial ecosystems. Microbiome. 2018; 6(1):12. Epub 2018/01/18. https://doi.org/10.1186/s40168-017-0393-0 PMID: 29335027; PubMed Central PMCID: PMC5769346.

90. Marie Booth J, Fusi M, Marasco R, Michoud G, Fodelianakis S, Merlino G, et al. The role of fungi in heterogeneous sediment microbial networks. Sci Rep. 2019; 9(1):7537. Epub 2019/05/19. https://doi.org/10.1038/s41598-019-43980-3 PMID: 31101834; PubMed Central PMCID: PMC6525233.

91. Deveau A, Bonito G, Uehling J, Paoletti M, Becker M, Bindschedler S, et al. Bacterial-fungal interactions: ecology, mechanisms and challenges. FEMS Microbiol Rev. 2018; 42(3):335–52. Epub 2018/02/23. https://doi.org/10.1093/femsre/fuy008 PMID: 29471481.

92. Kastner M. Evidence for two distinct hydrothermal systems in the Guaymas Basin. Eds. Curray J. R., Blakeslee J., Platt L.W., Stout L.N., Moore D.G., Aguayo J.E., et al. Washington, DC (U.S. Government Printing Office). In Initial Reports of the Deep Sea Drilling Project. 1982;Vol 64: 1143–57.

93. Gieskes J, Kastner M, Einsele G, Kelts K, Niemitz J. Hydrothermal activity in the Guaymas Basin, Gulf of California: a synthesis. In Initial Reports of the Deep Sea Drilling Project, Vol. 64, eds Curray J. R., Blakeslee J, Platt L. W., Stout L. N., Moore D. G., and Aguayo J. E.et al. Washington, DC: U.S. Government Printing Office, 1159–1167. 1982.

94. Peterson LE. Evaluating fluid fluxes from deep-sea seepage habitats. Ph.D. Dissertation, Coastal Carolina University, 2019, 238 pp. 2019.

95. Zeilinger-Migsich S, Mukherjee P. Editorial: Fungus-fungus interactions. The Open Mycology Journal. 2014; 8:27.

96. Fukasawa Y, Savoury M, Boddy L. Ecological memory and relocation decisions in fungal mycelial networks: responses to quantity and location of new resources. ISME J. 2020; 14(2):380–8. Epub 2019/10/20. https://doi.org/10.1038/s41396-019-0536-3 PMID: 31628441; PubMed Central PMCID: PMC6976561.

97. Fricker MD, Heaton LLM, Jones NS, Boddy L. The Mycelium as a Network. Microbiol Spectr. 2017; 5 (3). Epub 2017/05/20. https://doi.org/10.1128/microbiolspec.FUNK-0033-2017 PMID: 28524023.

98. Steele JA, Countway PD, Xia L, Vigil PD, Beman JM, Kim DY, et al. Marine bacterial, archaeal and protistan association networks reveal ecological linkages. ISME J. 2011; 5(9):1414–25. Epub 2011/03/25. https://doi.org/10.1038/ismej.2011.24 PMID: 21430787; PubMed Central PMCID: PMC3160682.

99. Bowsher AW, Benucci GMN, Bonito G, Shade A. Seasonal Dynamics of Core Fungi in the Switch-grass Phyllosphere, and Co-Occurrence with Leaf Bacteria. Phytobiomes Journal. 2021; 5(1):60–8. https://doi.org/10.1094/pbiomes-07-20-0051-r

100. Vigneron A, Cruaud P, Roussel EG, Pignet P, Caprais JC, Callac N, et al. Phylogenetic and functional diversity of microbial communities associated with subsurface sediments of the Sonora Margin, Guaymas Basin. PLoS One. 2014; 9(8):e104427. https://doi.org/10.1371/journal.pone.0104427 PMID: 25099369; PubMed Central PMCID: PMC4123917.

101. Lee C, Wakeham S, Arnosti C. Particulate Organic Matter in the Sea: The Composition Conundrum. AMBIO: A Journal of the Human Environment. 2004; 33(8). https://doi.org/10.1579/0044-7447-33.8.565 PMID: 15666690

102. Orsi WD. Ecology and evolution of seafloor and subseafloor microbial communities. Nat Rev Microbiol. 2018; 16(11):671–83. Epub 2018/07/04. https://doi.org/10.1038/s41579-018-0046-8 PMID: 29967420.

103. Steliga T. The role of fungi in biodegradation of petroleum hydrocarbons in drill waste. Pol J Environ Stud. 2012; 21:471–9.

104. Nasrawi HA. Biodegradation of Crude Oil by Fungi Isolated from Gulf of Mexico. Journal of Bioremediation & Biodegradation. 2012; 03(04). https://doi.org/10.4172/2155-6199.1000147

105. Álvarez-Barragán J, Cravo-Laureau C, Wick L, Duran R. Fungi in PAH-contaminated marine sediments: Cultivable diversity and tolerance capacity towards PAH. Marine Polution Bulletin. 2021; 164:112082. https://doi.org/10.1016/j.marpolbul.2021.112082 PMID: 33524832

106. Liu CH, Huang X, Xie TN, Duan N, Xue YR, Zhao TX, et al. Exploration of cultivable fungal communities in deep coal-bearing sediments from approximately 1.3 to 2.5 km below the ocean floor. Environ Microbiol. 2017; 19(2):803–18. Epub 2016/12/29. https://doi.org/10.1111/1462-2920.13653 PMID: 28028923.

107. Zain Ul Arifeen M, Chu C, Yang X, Liu J, Huang X, Ma Y, et al. The anaerobic survival mechanism of Schizophyllum commune 20R-7-F01, isolated from deep sediment 2 km below the seafloor. Environ Microbiol. 2021; 23(2):1174–85. Epub 2020/11/21. https://doi.org/10.1111/1462-2920.15332 PMID: 33215844.

108. Prince R. The microbiology of marine oil spill bioremediation. In Petroleum Microbiology. Oliver B, Magot M(eds.), Washington, D.C., ASM Press, 317–335. 2005.

109. Didyk BM, Simoneit BRT. Hydrothermal oil of Guaymas Basin and implications for petroleum formation mechanisms. Nature. 1989; 342:65–9.

110. Seewald JS, Seyfried WE, Thornton EC. Organic-rich sediment alteration: an experimental and theoretical study at elevated temperatures and pressures. Appl Geochem. 1990; 5:193–209.

111. Grossart H-P, Wurzbacher C, James TY, Kagami M. Discovery of dark matter fungi in aquatic ecosystems demands a reappraisal of the phylogeny and ecology of zoosporic fungi. Fungal Ecology. 2016; 19:28–38. https://doi.org/10.1016/j.funeco.2015.06.004

112. Gleason F, Küpper F, Amon J, Picard K, Gachon C, Marano A, et al. Zoosporic true fungi in marine ecosystems: a review. Marine Freshwater Res. 2011; 62:383–93.

113. Zhang T, Wang NF, Zhang YQ, Liu HY, Yu LY. Diversity and distribution of fungal communities in the marine sediments of Kongsfjorden, Svalbard (High Arctic). Sci Rep. 2015; 5:14524. Epub 2015/10/27. https://doi.org/10.1038/srep14524 PMID: 26494429; PubMed Central PMCID: PMC4615975.

114. Letcher PM, Powell MJ, Barr DJ, Churchill PF, Wakefield WS, Picard KT. Rhizophlyctidales—a new order in Chytridiomycota. Mycol Res. 2008; 112(Pt 9):1031–48. Epub 2008/08/15. https://doi.org/10.1016/j.mycres.2008.03.007 PMID: 18701267.

115. Longcore J, Barr D, Desaulniers N. Powellomyces, a new genus in the Spizellomycetales. Can J Bot. 1995; 73:1385–90.

116. Stoeck T, Epstein S. Novel eukaryotic lineages inferred from small-subunit rRNA analyses of oxygen-depleted marine environments. Appl Environ Microbiol. 2003; 69(5):2657–63. Epub 2003/05/07. https://doi.org/10.1128/AEM.69.5.2657-2663.2003 PMID: 12732534; PubMed Central PMCID: PMC154554.

117. Freeman KR, Martin AP, Karki D, Lynch RC, Mitter MS, Meyer AF, et al. Evidence that chytrids dominate fungal communities in high-elevation soils. Proc Natl Acad Sci U S A. 2009; 106(43):18315–20. Epub 2009/10/15. https://doi.org/10.1073/pnas.0907303106 PMID: 19826082; PubMed Central PMCID: PMC2775327.

118. Luo Y, Wei X, Yang S, Gao YH, Luo ZH. Fungal diversity in deep-sea sediments from the Magellan seamounts as revealed by a metabarcoding approach targeting the ITS2 regions. Mycology. 2020; 11(3):214–29. Epub 2020/10/17. https://doi.org/10.1080/21501203.2020.1799878 PMID: 33062383; PubMed Central PMCID: PMC7534268.

119. Youssef NH, Couger MB, Struchtemeyer CG, Liggenstoffer AS, Prade RA, Najar FZ, et al. The genome of the anaerobic fungus Orpinomyces sp. strain C1A reveals the unique evolutionary history of a remarkable plant biomass degrader. Appl Environ Microbiol. 2013; 79(15):4620–34. Epub 2013/05/28. https://doi.org/10.1128/AEM.00821-13 PMID: 23709508; PubMed Central PMCID: PMC3719515.

120. Gruninger RJ, Puniya AK, Callaghan TM, Edwards JE, Youssef N, Dagar SS, et al. Anaerobic fungi (phylum Neocallimastigomycota): advances in understanding their taxonomy, life cycle, ecology, role and biotechnological potential. FEMS Microbiol Ecol. 2014; 90(1):1–17. Epub 2014/07/22. https://doi.org/10.1111/1574-6941.12383 PMID: 25046344.

121. Boxma B, Voncken F, Jannink S, van Allen T, Akhmanova A, van Weelden S, et al. The anaerobic chytridiomycete fungus Piromyces sp. E2 produces ethanol via pyruvate:formate lyase and an alcohol dehydrogenase E. Mol Microbiol. 2004; 51:1389–99. https://doi.org/10.1046/j.1365-2958.2003.03912.x PMID: 14982632

122. Teunissen M, Op den Camp H, Orpin C, Huis in't Veld J, Vogels G. Comparison of growth characteristics of anaerobic fungi isolated from ruminant and non-ruminant herbivores during cultivation in a defined medium. J gen Microbiol. 1991; 137:1401–8. https://doi.org/10.1099/00221287-137-6-1401 PMID: 1919514

123. Drake H, Ivarsson M, Bengtson S, Heim C, Siljestrom S, Whitehouse MJ, et al. Anaerobic consortia of fungi and sulfate reducing bacteria in deep granite fractures. Nat Commun. 2017; 8(1):55. Epub 2017/07/06. https://doi.org/10.1038/s41467-017-00094-6 PMID: 28676652; PubMed Central PMCID: PMC5496868.

124. Drake H, Ivarsson M, Heim C, Snoeyenbos-West O, Bengtson S, Belivanova V, et al. Fossilized anaerobic and possibly methanogenesis-fueling fungi identified deep within the Siljan impact structure, Sweden. Communications Earth & Environment. 2021; 2(1). https://doi.org/10.1038/s43247-021-00107-9

125. Robert V, Cardinali G, Casadevall A. Distribution and impact of yeast thermal tolerance permissive for mammalian infection. BMC Biol. 2015; 13:18. Epub 2015/03/13. https://doi.org/10.1186/s12915-015-0127-3 PMID: 25762372; PubMed Central PMCID: PMC4381509.

126. Pang KL, Guo SY, Chen IA, Burgaud G, Luo ZH, Dahms HU, et al. Insights into fungal diversity of a shallow-water hydrothermal vent field at Kueishan Island, Taiwan by culture-based and metabarcoding analyses. PLoS One. 2019; 14(12):e0226616. Epub 2019/12/31. https://doi.org/10.1371/journal.pone.0226616 PMID: 31887170; PubMed Central PMCID: PMC6936883.

127. Burgaud G, Le Calvez T, Arzur D, Vandenkoornhuyse P, Barbier G. Diversity of culturable marine filamentous fungi from deep-sea hydrothermal vents. Environ Microbiol. 2009; 11(6):1588–600. Epub 2009/02/26. https://doi.org/10.1111/j.1462-2920.2009.01886.x PMID: 19239486.